



## Sensitivity of simulated historical burned area to environmental and anthropogenic controls: A comparison of seven fire models

Lina Teckentrup<sup>1</sup>, Sandy P. Harrison<sup>2</sup>, Stijn Hantson<sup>3</sup>, Angelika Heil<sup>1</sup>, Joe R. Melton<sup>4</sup>, Matthew Forrest<sup>5</sup>, Fang Li<sup>6</sup>, Chao Yue<sup>7</sup>, Almut Arneth<sup>3</sup>, Thomas Hickler<sup>5</sup>, Stephen Sitch<sup>8</sup>, and Gitta Lasslop<sup>1,5</sup>

<sup>1</sup>Max Planck Institute for Meteorology, 20146 Hamburg, Germany

<sup>2</sup>School of Archaeology, Geography and Environmental Sciences (SAGES), University of Reading, Whiteknights, Reading, UK

<sup>3</sup>Karlsruhe Institute of Technology, Institute of Meteorology and Climate Research, Atmospheric Environmental Research, 82467 Garmisch-Partenkirchen, Germany

<sup>4</sup>Climate Research Division, Environment Canada, Victoria, BC, V8W 2Y2, Canada

<sup>5</sup>Senckenberg Biodiversity and Climate Research Institute (BiK-F), 60325 Frankfurt am Main, Germany

<sup>6</sup>International Center for Climate and Environmental Sciences, Institute of Atmospheric Physics, Chinese Academy of Sciences

<sup>7</sup>Laboratoire des Sciences du Climat et de l'Environnement–Institute Pierre Simon Laplace, Commissariat à l'Énergie Atomique et aux Énergies Alternatives (CEA)–Centre National de la Recherche Scientifique (CNRS)–Université de Versailles Saint Quentin

<sup>8</sup>College of Life and Environmental Sciences, University of Exeter

**Correspondence:** Gitta Lasslop ([gitta.lasslop@senckenberg.de](mailto:gitta.lasslop@senckenberg.de))

**Abstract.** Understanding how fire regimes change over time is of major importance for understanding their future impact on the Earth system, including society. Large differences in simulated burned area between fire models show that there is substantial uncertainty associated with modelling global change impacts on fire regimes. We draw here on sensitivity simulations made by seven global dynamic vegetation models participating in the Fire Model Intercomparison Project (FireMIP) to understand how differences in models translate into differences in fire regime projections. The sensitivity experiments isolate the impact of the individual drivers of fire, which are prescribed in the simulations. Specifically these drivers are atmospheric CO<sub>2</sub>, population density, land-use change, lightning and climate.

The seven models capture spatial patterns in burned area. However, they show considerable differences in the burned area trends since 1900. We analyse the trajectories of differences between the sensitivity and reference simulation to improve our understanding of what drives the global trend in burned area. Where it is possible, we link the inter-model differences to model assumptions.

Overall, these analyses reveal that the strongest differences leading to diverging trajectories are related to the way anthropogenic ignitions and suppression, as well as the effects of land-use on vegetation and fire, are incorporated in individual models. This points to a need to improve our understanding and model representation of the relationship between human activities and fire to improve our abilities to model fire for global change applications. Only two models show a strong response to CO<sub>2</sub> and the response to lightning on global scale is low for all models. The sensitivity to climate shows a spatially heterogeneous response and globally only two models show a significant trend. It was not possible to attribute the climate-induced changes in



burned area to model assumptions or specific climatic parameters. However, the strong influence of climate on the inter-annual variability in burned area, shown by all the models, shows that we need to pay attention to the simulation of fire weather but also meteorological influences on biomass accumulation and fuel properties in order to better capture extremes in fire behavior.

*Copyright statement.*

## 5 1 Introduction

About 4% of the global vegetated area burns each year (Giglio et al., 2013), but between 30-40% of the land surface is affected by fire regularly (Chapin et al., 2002; Chuvieco et al., 2008). Thus, over large parts of the world, wildfires are an important cause of vegetation disturbance, and regulate ecosystem functioning, biodiversity and carbon storage (Bond et al., 2005; Hantson et al., 2016). Fire has strong impacts on climate through changing land surface properties, atmospheric chemistry and hence radiative forcing, as well as biogeochemical cycling (Bowman et al., 2009; Randerson et al., 2012; Ward et al., 2012; Yue et al., 2016; Li and Lawrence, 2017; Li et al., 2017). Analyses based on observations of the pre-industrial period suggest that the contribution of fire to the overall climate-carbon-cycle feedback is substantial ( $5.6 \pm 3.2$  ppm CO<sub>2</sub> per degree of land temperature change; Harrison et al., 2018). In addition to these consequences for the Earth System, wildfires directly impact society and economy (Gauthier et al., 2015) and human health can be seriously impaired (Johnston et al., 2012; Finlay et al., 2012).

Given the various impacts that fire has on natural and human systems, it is important to understand what controls the occurrence of wildfires and to know how fire regimes might change in the future. The fire model intercomparison project (FireMIP, Hantson et al., 2016; Rabin et al., 2017a) provides simulations for a systematic comparison of fire-model behaviour based on outputs from a large range of multiple model runs with identical forcing inputs. Sensitivity simulations were conducted for individual forcings, specifically CO<sub>2</sub>, population density, land-use change, lightning and climate.

Based on current process understanding these drivers may influence burned area in the following ways:

Increasing atmospheric CO<sub>2</sub> concentration leads to increases in net primary production (Hickler et al., 2008; Knorr et al., 2016) and decreased stomatal conductance reduces the plant transpiration (Morison, 1985). It can lead to changes in vegetation composition ('woody thickening'; Wigley et al., 2010; Bond and Midgley, 2012; Buitenwerf et al., 2012) because C<sub>3</sub> plants are generally more competitive than C<sub>4</sub> plants under higher CO<sub>2</sub> (e.g. Ehleringer and Björkman, 1977; Ehleringer et al., 1997; Wand et al., 2001; Sage and Kubien, 2007). The impact of these various changes on burned area is complex. Increased productivity can lead to increased fuel availability, which can lead to increased burned area in water- and fuel-limited regions (Kelley and Harrison, 2014). On the other hand, decreased stomatal conductance can lead to increased soil and fuel moisture contents and hence to a reduction in burned area in more humid regions. Woody thickening can lead to a reduction in burned area through changing the nature of fuel loads (Kelley and Harrison, 2014).

There is still controversy about whether humans increase or decrease fire overall: Although there is broad agreement that



humans suppress fires in regions with high population density, observational studies are less clear about what happens in areas of low population density and show both increases or decrease due to human activities (see for instance Marlon et al., 2008; Bowman et al., 2011; Marlon et al., 2013; Vanni re et al., 2016; Andela et al., 2017; Balch et al., 2017). Studies of the covariation between population density and number of fires have shown that increasing population density leads to an increase in the number of ignitions or in the number of individual fires until peaking at inter-mediate population densities and drop subsequently (Syphard et al., 2009; Archibald et al., 2010). The increase in burned area for low population density is expected to differ from the one found for number of fires as the largest fires occur in unpopulated areas (Hantson et al., 2015a) and burned area can be expressed as number of fires times fire size. Global analysis find that the net effect of population density is a decrease in burned area (Bistinas et al., 2014; Knorr et al., 2014), with high uncertainties for low population density if the method allows for non-monotonic relationships (Knorr et al., 2014). Regional analysis tends to confirm this, but positive relationships between burned area and population density have been shown, for instance, for the least disturbed areas in the USA (Parisien et al., 2016).

Fire was used to manage croplands in pre-industrial times (e.g. Dumond, 1961; Otto and Anderson, 1982; Johnston, 2003) and it is still common practice in mainly in non-industrialized areas (i.e. Sub-Saharan Africa, parts of South East Asia, Indonesia and Latin America; e.g. Conklin, 1961; Rasul and Thapa, 2003). However fires in agricultural areas are common on all over the world (Korontzi et al., 2006). The influence of land-use on fire on global scale is not well studied. Severe data gaps and an unsatisfactory level of understanding characterize our knowledge on how humans use fire in land management (Erb et al., 2017). Analysis of satellite data indicate a decrease of burned area (Bistinas et al., 2014; Andela and van der Werf, 2014) and fire size (Hantson et al., 2015b) with increases in cropland fraction. Fires on pastures contribute over 40% of the global burned area (Rabin et al., 2015). Analysis of global datasets find an increase of burned area with increases in pasture cover fraction Bistinas et al. (2014) but reduced burned area on intensely grazed areas (Andela et al., 2017).

Lightning is the main source of natural ignitions (Scott et al., 2014). It is connected to convective activity and is therefore expected to change with global warming (Krause et al., 2014). Most of total burned area in boreal regions, for example, results from a few large fires (Stocks et al., 2002); these large fires are frequently ignited by lightning (Peterson et al., 2010). Veraverbeke et al. (2017) have shown that lightning ignitions drive interannual variability as well as long-term trends of the ignitions in boreal regions.

Climate can influence burned area through weather conditions and vegetation (Bistinas et al., 2014; Forkel et al., 2017). Weather conditions (precedent precipitation, temperature and wind speeds) influence fuel drying, while wind speed affects the rate of fire spread (Harrison et al., 2010; Scott et al., 2014). Fuel loads and vegetation type are also driven by climate and both strongly determine fire occurrence (Chuvieco et al., 2008; Pettinari and Chuvieco, 2016). As fires are limited at low moisture conditions due to low productivity and therefore insufficient fuel, and at high moisture conditions due to the fuel being too wet to burn, the highest burned areas are found in areas with medium moisture conditions (Krawchuk and Moritz, 2011). There is no obvious controversy in literature on how specific climatic factors drive fire. However, the strength of single factors and balance between factors, e.g. weather vs. vegetation, is still uncertain and varies spatially (Forkel et al., 2017). Fire models are sensitive to the meteorological forcing, different forcing datasets already lead to large differences in simulated burned area (Rabin et al.,



2017a; Lasslop et al., 2014). Wind speed for instance strongly varies between datasets and although wind speed is an obvious driver of fire spread, it is difficult to extract this influence on the spatial resolution of global models (Lasslop et al., 2015).

Fire-enabled vegetation models generally simulate observed global patterns of burned area and fire emissions reasonably well (Kloster et al., 2010; Prentice et al., 2011; Li et al., 2012; Lasslop et al., 2014; Yue et al., 2014), but there are large differences  
5 between models in terms of regional patterns, fire seasonality and interannual variability, and historical trends (Kelley et al., 2013; Andela et al., 2017). A recent evaluation of the FireMIP models indicates that the relationship with climatic parameters is captured well by models, the response to human factors is captured by some models and the response to vegetation productivity needs refinement for most models (Forkel et al., 2019).

In this study we briefly assess how well the FireMIP models simulated present day burned area. We then document how  
10 simulated burned area responds to individual forcing factors and relate inter-model differences of the burned area response to differences in model assumptions or parametrisation. We finally discuss the model limitations and implications of our results for model development and application.

## 2 Methods

The baseline FireMIP experiment (SF1) is a transient simulation from 1700–2013, in which CO<sub>2</sub>, population density, land–  
15 use, lightning, and climate change through time according to prescribed datasets (see Rabin et al. (2017a) for details of the experimental protocol). The five sensitivity experiments (SF2) are designed to isolate differences in model behaviour associated with individual forcing factors. The model inputs and setup are the same as in SF1, but one of the forcings is kept constant throughout the simulation in each experiment (see tab. 1). Thus, for example, in SF2\_CO2, population density, land–use, lightning and climate inputs change each year, but CO<sub>2</sub> is held constant at 277.33 ppm for the whole of the simulation. Not all  
20 models performed every sensitivity experiment due to limitations in model structure (see tab. 2). Two of the models (CLASS–CTEM and CLM) started the simulations later than the others (1861 and 1850, respectively). Since our analyses are confined to differences in behavior during the 20th century, this difference in the length of the simulations between the models should have little impact.



**Table 1.** Overview over the sensitivity experiments conducted by FireMIP-models (Rabin et al., 2017a). Rptd indicates the forcing was repeated over the given years. SF2\_CO2 stands for fixed CO2, SF2\_FPO for fixed population density, SF2\_FLA for fixed land use, SF2\_FLI for fixed lightning, and SF2\_CLI for fixed climate.

Driving factor	Sensitivity Experiments				
	SF2_CO2	SF2_FPO	SF2_FLA	SF2_FLI	SF2_CLI
CO <sub>2</sub>	277.33 ppm	transient	transient	transient	transient
Population density (PD)	transient	Fixed Year 1	transient	transient	transient
Land-use change (LUC)	transient	transient	Fixed Year 1	transient	transient
Lightning	transient	transient	transient	Rptd: 1901–1920	transient
Climate	transient	transient	transient	transient	Rptd: 1901–1920

**Table 2.** Sensitivity experiments conducted by FireMIP models.

Model	Sensitivity Experiments				
	SF2_CO2	SF2_FPO	SF2_FLA	SF2_FLI	SF2_CLI
CLASS–CTEM	x	x	x	x	x
CLM	x	x	x	x	x
INFERNO	x	x	x		
JSBACH–SPITFIRE	x	x	x	x	x
LPJ–GUESS–SIMFIRE–BLAZE	x	x	x		x
LPJ–GUESS–SPITFIRE	x	x	x	x	x
ORCHIDEE–SPITFIRE	x	x	x	x	x

Detailed model descriptions can be found in the corresponding literature listed in table A1.

## 2.1 Data processing and analysis of simulation results

Our analyses of the SF1 and SF2 simulations focus on the simulation of burned area but are complemented by effects on vegetation carbon pools for the SF2\_CO2 simulation. We focus on the time series of global burned area over the historical simulation and the spatial patterns of differences in burned area between 1900 and 2013, as in this period all forcings are transient. Annual global values are an area weighted average using the grid cell area. We quantify the sensitivity of the models



to each driving factor using the relative difference in burned area between the baseline and the respective sensitivity experiment  $((SF1-SF2_i)/SF2_i)$ , with  $i$  in CO<sub>2</sub>, FPO, FLA, FLI, CLI). We use the climate data operators (CDO version 2018: Climate Data Operators. Available at: <http://www.mpimet.mpg.de/cdo>) to process and remap the simulated outputs. We test the relative difference time series for trends over the period from 1900 to 2013 using the Mann-Kendall test, implemented in the R package Kendall (McLeod, 2011). We quantify the global trend as the slope of a linear regression and summarize the spatial distribution of trends by quantifying the area with significant positive trends and the area with significant negative trends. Due to a postprocessing error, INFERNO lacks two years in SF2\_CO<sub>2</sub> (2002 and 2003).

## 2.2 Model-data comparison

To evaluate the realism of the simulations of burned area, we compare the simulated burned area with remote sensing data products. We used three satellite products: GFED4 (Giglio et al., 2013), GFED4s (Randerson et al., 2012) and FireCCI50 (Chuvieco et al., 2018). These three data sets use different retrieval algorithms, which cause differences in spatial and temporal patterns in burned area (Hantson et al., 2016; Humber et al., 2018). Since there is no agreement about which is most reliable, using all three products provides a measure of the uncertainty in the observations. For the comparison we use temporally averaged burned fraction for the years 2001–2013, which is the interval common to all three satellite data sets and the model simulations. For this comparison, we scale the model outputs to the lowest model resolution (CLASS-CTEM: 2.8125 x 2.8125°) with first order conservative remapping. Due to the strongly skewed distribution of burned area fraction we apply a square root transformation on both observations and model output. We quantify the agreement between models and observations with the Pearson correlation coefficient (see tab. 3).

In spite of major advances in mapping burned area based on satellite data, these data products include major uncertainties. GFED4 and FireCCI50 provide uncertainty estimates for the burned area. Applying Gaussian error propagation, which assumes that errors are independent and normally distributed, yields uncertainty estimates of 0.01 and 0.2 % of the global burned area, which is certainly an underestimation. The assumptions of normal distribution and independence are likely violated. The spread between global burned area data sets is probably a more realistic estimate. Since all the products rely on the MODIS sensor, this approach will, however, also not capture the full uncertainty. Nevertheless, to investigate the effect of data quality in the observations on the model-data comparison we use the burned area product uncertainty estimates (aggregated to model resolution assuming independence) to group the observations into points with low, medium and high uncertainty (low: within the 0–33rd percentile, medium: within the 33rd–66th percentile, and high: within the 66th–99th percentile of the relative uncertainty estimates = uncertainty / burned area). We then compute the correlations for data points with low, medium and high uncertainty separately.



### 3 Results and discussion

#### 3.1 Evaluation of the baseline experiment

The models show magnitudes of annual global burned area between 354–530 Mha/yr for present day. This is comparable to the estimates obtained from the satellite products, which range from 345–480 Mha/yr (see fig. 1, tab. 3). The correlation coefficients between all of the simulations and the satellite observations are reasonable, with values ranging from 0.51 (CLASS–CTEM, GFED4s) to 0.8 (ORCHIDEE–SPITFIRE, GFED4; see tab. 3). In general, the correlations with GFED4 are highest and with GFED4s lowest for almost all models - which may reflect the fact that most models do not explicitly simulate agricultural fires or may reflect an overestimation or not sufficiently precise estimation of the contribution of such fires to burned area in the GFED4s data set. The correlation coefficients strongly decrease with increasing observational relative uncertainty (see tab. A2), showing that part of the mismatch in the spatial patterns between simulations and observations is a consequence of uncertainties in the satellite products themselves. The FireMIP models simulate the broad scale patterns in burned area reasonably well (see fig. A1), with maxima in the major fire-affected regions of the Sahel, southern Africa, northern Australia and the western USA. All of the models tend to overestimate the burned area in South America and also in the temperate regions of the USA.

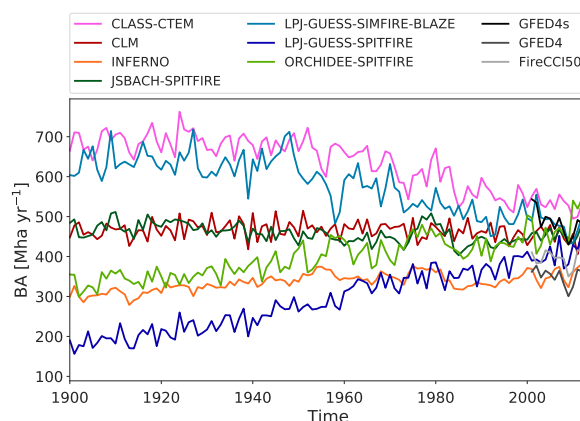


**Figure 1.** Annual global burned area (BA) in  $\text{Mha yr}^{-1}$  for all FireMIP-models for 1900–2013 for the baseline experiment SF1.



**Table 3.** Global burned area averaged over 2001–2013 in Mha yr<sup>-1</sup> and the Pearson correlation coefficients between the baseline experiment SF1 for all FireMIP-models and the respective observation data. Due to the skewed distribution of burned area, we use a square root transformation on both model and observations. All correlation coefficients are significant (p-value < 0.001).

Model	Burned Area (Mha yr <sup>-1</sup> )	R(GFED4, model)	R(GFED4s, model)	R(FireCCI50, model)
CLASS–CTEM	531	0.58	0.51	0.56
CLM	451	0.73	0.68	0.74
INFERNO	354	0.70	0.64	0.69
JSBACH–SPITFIRE	455	0.66	0.57	0.62
LPJ–GUESS–SIMFIRE–BLAZE	482	0.67	0.60	0.62
LPJ–GUESS–SPITFIRE	404	0.55	0.56	0.59
ORCHIDEE–SPITFIRE	474	0.80	0.72	0.79
GFED4	345			
GFED4s	480			
FireCCI50	389			

The simulated trend in burned area of the historical reference simulation differs between the models (see fig. 1). All models, except CLM, have a significant trend over the time series from 1900–2013 (see tab. 4). Models that have a relatively high total burned area initially (LPJ–GUESS–SIMFIRE–BLAZE, CLASS–CTEM) show a decline in burned area over the 20th century. Most models that have a low burned area (INFERNO, ORCHIDEE–SPITFIRE, LPJ–GUESS–SPITFIRE) show an increasing trend. JSBACH–SPITFIRE and CLM have intermediate levels in burned area and show a weak decreasing trend over the 20th century. Only half of the models show a decline in burned area after 2000 CE (see Andela et al., 2017). The global decline in satellite data is strongly dominated by savanna ecosystems and the spatial pattern of trends is very heterogeneous (Andela et al., 2017). The short length of the satellite record leads to uncertainties in the trends, which are in most regions statistically not significant (Andela et al., 2017). Few datasets exist for the longer term trend. Charcoal data are a proxy for fire occurrence over longer time scales (Marlon et al., 2008, 2016). These charcoal records show a global decrease in biomass burning over most of the 20th century (Marlon et al., 2008, 2016), which is consistent with carbon monoxide data from ice-core records (Wang et al., 2010). However, the charcoal records appear to show an increase in burning since 2000 CE, contrary to the decline shown by satellite-based records of burned area (Andela et al., 2017). This discrepancy might reflect sampling or taphonomic issues of the charcoal record. For instance the continents that contribute most to the global burned area (Africa) is heavily undersampled. A recently developed fire emissions dataset (van Marle et al., 2017) merges information from satellites, charcoal records, airport visibility records and if no other information was available uses simulation results of the FireMIP models. This dataset is not included here as it is partly based on the simulations of the models used in this study and as it does not provide estimates of burned area. A decline in global burned area over the 20th century might be more realistic than the increase shown by several models. Further evaluation of historical trends in fire proxies and longer satellite time series will help to gain more confidence



in observed trends of fire regimes. The better understanding of the drivers of simulated trends that we provide below can inform us on how certain trends can be achieved in models.

**Table 4.** Trends (slope of a linear regression) in annual global burned area for the years 1900-2013 for the baseline experiment SF1 ([Mha yr<sup>-1</sup>]) and relative difference timeseries of annual burned area between the baseline experiment SF1 and the sensitivity experiments SF2 [% year<sup>-1</sup>] (see tab. 1). Bold values indicate significance based on a Mann-Kendall test (p-value < 0.05). Experiments that are not available for specific models are indicated with n.a..

Model	Sensitivity Experiments					
	SF1	SF2_CO2	SF2_FPO	SF2_FLA	SF2_FLI	SF2_CLI
CLASS-CTEM	<b>-1.762</b>	<b>-0.009</b>	<b>-0.063</b>	<b>-0.160</b>	0.000	0.025
CLM	-0.138	<b>0.016</b>	<b>-0.156</b>	<b>-0.013</b>	-0.010	<b>0.028</b>
INFERNO	<b>0.433</b>	<b>0.026</b>	<b>-0.123</b>	<b>0.094</b>	n.a.	n.a.
JSBACH-SPITFIRE	<b>-0.321</b>	<b>0.139</b>	<b>0.010</b>	<b>-0.141</b>	<b>-0.017</b>	0.028
LPJ-GUESS-SIMFIRE-BLAZE	<b>-1.782</b>	<b>-0.015</b>	<b>-0.129</b>	<b>-0.204</b>	n.a.	<b>0.054</b>
LPJ-GUESS-SPITFIRE	<b>2.270</b>	<b>0.242</b>	<b>0.441</b>	<b>0.686</b>	<b>0.005</b>	-0.060
ORCHIDEE-SPITFIRE	<b>1.338</b>	<b>0.011</b>	<b>0.120</b>	<b>0.222</b>	<b>0.073</b>	0.002

### 3.2 Sensitivity of models to individual drivers

There are large differences in sign and magnitude between models in the temporal response of global burned area from 1900–2013 to each individual driving factor when compared to the baseline experiment (see fig. 2, tab. 4). Population density (SF2\_FPO) and land-use change (SF2\_FLA) cause the largest inter-model spread in trends (slope between -0.156 and 0.441 % year<sup>-1</sup> and between -0.204 and 0.686 % year<sup>-1</sup>, respectively), all trends are statistically significant (see tab. 4, fig. 2 b and c). For SF2\_CO2 all models have a significant trend, however, only LPJ-GUESS-SPITFIRE and JSBACH-SPITFIRE have a clear positive trend (> 0.13 % year<sup>-1</sup>), for all other models the slope is close to zero (< 0.03 % year<sup>-1</sup>; see tab. 4, fig. 2 a). The differences between models are increasing over the 20th century for these first three experiments. The response to changes in lightning and climate generally shows much smaller trends: only two models have a significant trend for climate, with increases in burned area due to changing climate (0.054 and 0.028 % year<sup>-1</sup>). Three models show significant (but inconsistent -0.017, 0.005 and 0.074 % year<sup>-1</sup>) trends for lightning (see tab. 4). The time series of differences between these latter two experiments and the baseline experiment show a strong inter-annual variability. This variability is stronger for climate (up to 30% in several years) than lightning (up to 20% for very few years and only one model; see fig. 2 d and e).

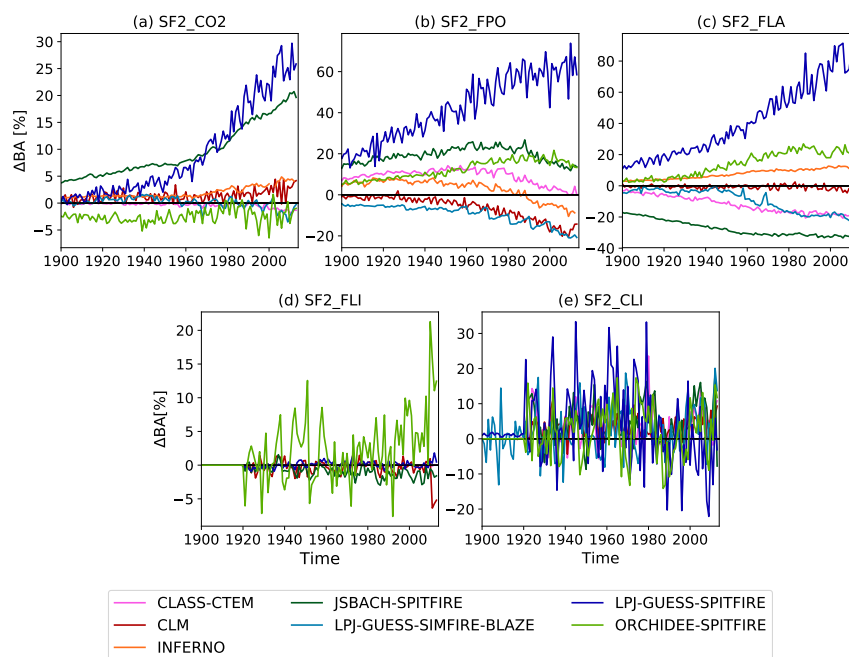


**Figure 2.** Relative difference in annual global burned area ( $\Delta BA$ ) in % across 1900 to 2013 between the baseline experiment SF1 and the sensitivity experiments SF2\_CO2 (a), SF2\_FPO (b), SF2\_FLA (c), SF2\_FLI (d) and (e) (see tab. 1). Note that the y-axis range differ between the panels.

The spatial patterns of trends in burned area are mostly heterogeneous (see supplement figures A3–A7). Limited areas of the world can dominate a global trend or the trends can cancel out when aggregating to the global burned area sum. A regional analysis is beyond the scope of this study, but we provide an alternative global view on the trends by quantifying the area affected by positive or negative trends (see fig. 3). This comparison shows that for most models larger areas show significant positive trends for the reference simulation (5 models), rising atmospheric CO<sub>2</sub> (5 models) and varying climate (all models), whereas there is no clear signal across models of either positive or negative trends across the models for the other simulations. For climate and lightning smaller areas show significant trends (see fig. 3). For ORCHIDEE– and LPJ–GUESS–SPITIFRE all factors but climate cause a significant positive trend globally (see tab. 4) and larger areas have positive trends for all factors, except lightning for LPJ–GUESS–SPITIFIRE (see fig. 3). On the other end of the model range LPJ–GUESS–SIMFIRE–BLAZE only shows a positive global trend for climate (see tab. 4), CO<sub>2</sub> and climate induce positive trends in larger areas than negative trends (see fig. 3).

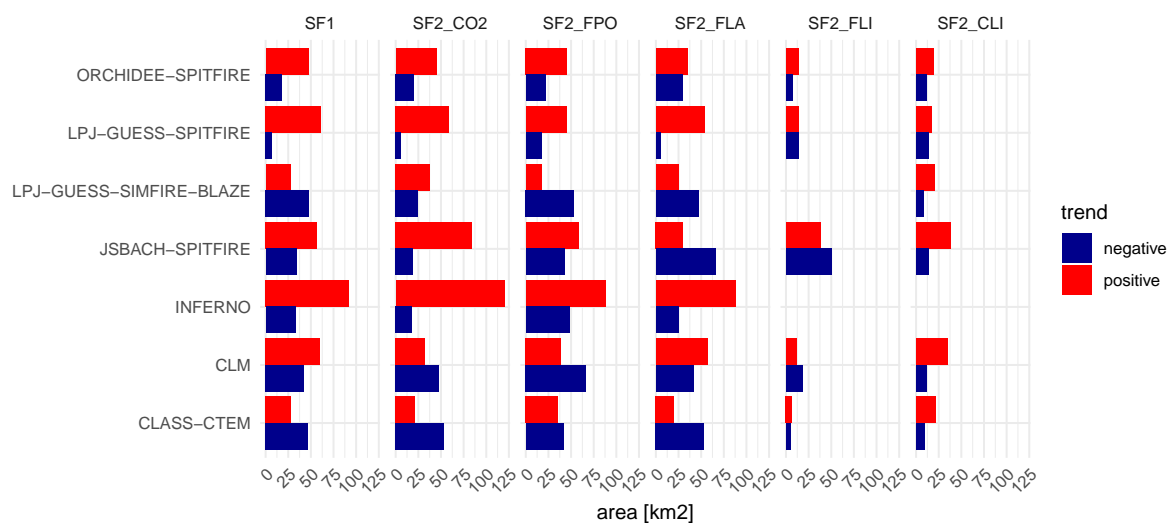


**Figure 3.** Area with a significant positive trend (red bar) or with a significant (Mann-Kendall test  $p < 0.05$ ) negative change (blue bar) in burned area fraction averaged over 1901–2013 for the baseline experiment SF1 and the sensitivity experiments SF2 (see tab. 1). Compare fig. A2 - A7.

In the following paragraphs we detail the inter-model differences and their causes for each sensitivity experiment.

### 3.2.1 Sensitivity of models to CO<sub>2</sub>

The overall changes in burned area in individual simulations as a result of atmospheric CO<sub>2</sub> changes are a complex response to multiple changes in vegetation: changes in land cover, fuel load, fuel characteristics and fuel moisture. Burned area can either increase due to higher availability of fuel loads or decrease due to changes in flammability caused by different fuel characteristics including moisture (Rabin et al., 2017a). The FireMIP-models react to increasing CO<sub>2</sub> in different ways: some models (JSBACH-SPITFIRE and LPJ-GUESS-SPITFIRE) show a strong increase in burned area, some (CLM and INFERNO) show a moderate increase, CLASS-CTEM shows a slight decrease, and LPJ-GUESS-SIMFIRE-BLAZE and ORCHIDEE-SPITFIRE show a non-monotonic response (see fig. 2, a). For all models, the trends over the 20th century are significant (see tab. 4).

We use changes in vegetation carbon to understand changes in fuel load and composition because information on the amount of fuel used within the fire models was not available for individual plant functional types (PFTs). All models show an increase in total vegetation biomass ('total', solid lines; see fig. 4). The response of specific types of vegetation carbon to increasing CO<sub>2</sub> varies between the vegetation models. The biomass of C<sub>3</sub> vegetation (trees and C<sub>3</sub> grasses) increases in all of the models. The biomass of C<sub>4</sub> grasses increases in CLASS-CTEM, INFERNO, and JSBACH-SPITFIRE, but does not change in ORCHIDEE-SPITFIRE. Since ORCHIDEE-SPITFIRE was run with fixed vegetation distribution, changes in the extent of different PFTs can be ruled out as a cause of changes in vegetation carbon. There is a decrease in burned area in regions with



abundant  $C_4$  grasses (Sahel and North Australia) in this model, suggesting that increased  $C_3$  tree biomass results in changes in flammability in these regions. The carbon stored in  $C_4$  grasses is reduced in response to increasing  $\text{CO}_2$  in CLM and LPJ-GUESS-SIMFIRE-BLAZE and is fairly constant in LPJ-GUESS-SPITFIRE. This can be a result of a decrease in  $C_4$  grass cover in LPJ-GUESS-SIMFIRE-BLAZE and LPJ-GUESS-SPITFIRE. However, since CLM was run with prescribed vegetation cover, the reduction in  $C_4$  carbon must reflect the fact that any increase in  $C_4$  grass biomass due to higher  $\text{CO}_2$  is offset by greater losses through burning due to the increased total fuel load.

CLM and LPJ-GUESS-SIMFIRE-BLAZE include an interactive nitrogen cycle, CLASS-CTEM a non-interactive nitrogen down-regulation. Effects of  $\text{CO}_2$  on vegetation biomass for these three models are therefore at the lower end of the model ensemble.

Soil moisture is used by several models to compute fuel moisture (see fig. 5). Soil moisture can be influenced by different atmospheric  $\text{CO}_2$  as reductions in stomatal conductance can lead to increases in soil moisture, whereas increases in LAI caused by increased biomass of increased tree cover lead to higher transpiration and therefore lower soil moisture. Soil moisture increases slightly in four models (INFERNO, CLASS-CTEM, CLM, JSBACH-SPITFIRE), and decreases slightly in ORCHIDEE-SPITFIRE. Only LPJ-GUESS-SPITFIRE shows a strong decrease (5% in global average) in soil moisture (see fig. 6)

Models which include fuel load and moisture effects through threshold functions (see fig. 5, CLASS-CTEM, INFERNO, CLM) tend to show muted responses. Decreases in burned area appear to be largely caused by increases in soil moisture or tree cover. Increases associated with increasing fuel load are limited to regions with low biomass. The balance between these effects differs between the models. CLASS-CTEM shows a small decrease in burned area globally, and the spatial pattern is dominated by areas with negative trends in burned area, but there are positive trends in dry regions (see fig. A3). The small global increase of burned area in INFERNO is likely related to increased fuel loads, negative trends in burned area only occur in the tropical regions (see fig. A3). INFERNO uses a constant burned area per PFT that is set to 0.6, 1.4 and 1.2  $\text{km}^2$  for trees, grass and shrubs. CLM shows increased global burned area, but increases are located in dry areas while the boreal regions show decreases. JSBACH-SPITFIRE and LPJ-GUESS-SPITFIRE respond to elevated  $\text{CO}_2$  with a strong increase in burned area, likely driven by increases in fuel load. LPJ-GUESS-SPITFIRE additionally shows a strong decrease in soil moisture, which might explain why this model shows the strongest increase in burned area. ORCHIDEE-SPITFIRE shows lower burned area in response to elevated atmospheric  $\text{CO}_2$  but the decreases are mainly localized in the regions with very high burned area (Sahel and Northern Australia; see fig. A3) and are likely driven by the increase in  $C_3$  woody biomass (see fig. 4) as SPITFIRE is very sensitive to the type of fuel (Lasslop et al., 2014). LPJ-GUESS-SIMFIRE-BLAZE shows an initial increase and a decrease in burned area at the end of the simulation. The spatial pattern is mixed, the decrease in  $C_4$  grass biomass indicates that woody thickening, either due to changes in land cover fraction or fuel composition is the reason for this reduction in burned area.

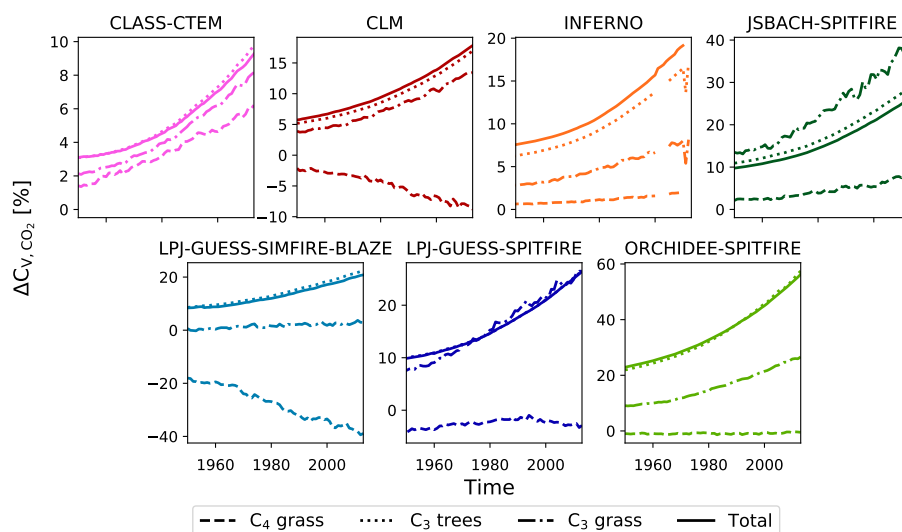


**Figure 4.** Relative difference in global carbon stored in  $C_4$  grasses (dashed lines), in  $C_3$  trees (dotted lines), in  $C_3$  grasses (dash-dotted lines) and in total global carbon stored in vegetation (solid lines) between the baseline experiment SF1 and the sensitivity experiment SF2\_CO2 (see tab. 1;  $C_{V,CO_2}$ ) for 1950–2013 in % (annual averages).  $C_4$  and  $C_3$  grasses as well as  $C_3$  trees only include natural PFTs (pastures and croplands excluded). Note that the y-axis limits differs between the panels. Due to a postprocessing error, INFERNO lacks two years (2002 and 2003).

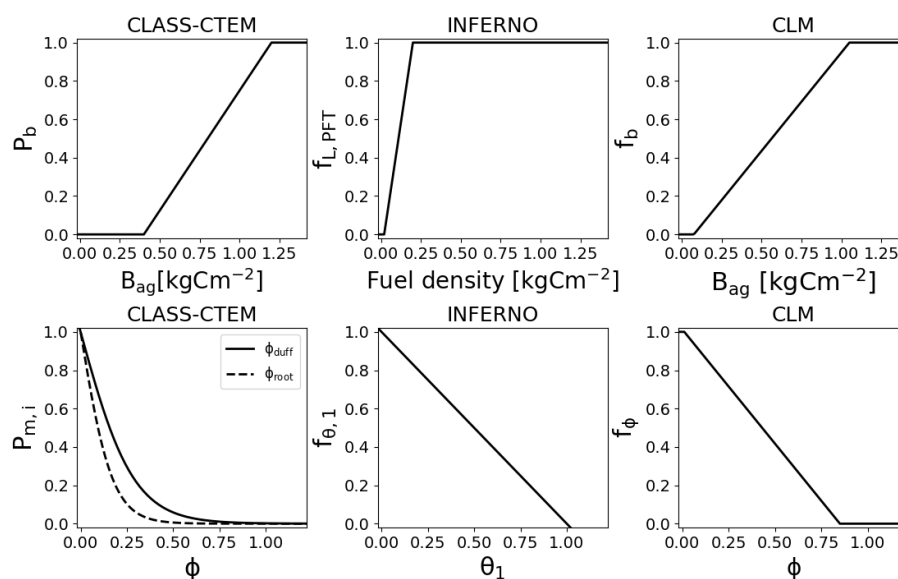


**Figure 5.** Impact of fuel load on the probability of fire ( $P_b$ ) for CLASS-CTEM, on the fuel load index ( $f_{L,PFT}$ ) for INFERNO and on fuel availability ( $f_b$ ) for CLM (top panels). Impact of soil moisture content and soil wetness on fire for CLASS-CTEM, CLM, and INFERNO (bottom panels). In order to facilitate comparability, the soil moisture function for CLM is scaled to the value range [0,1].

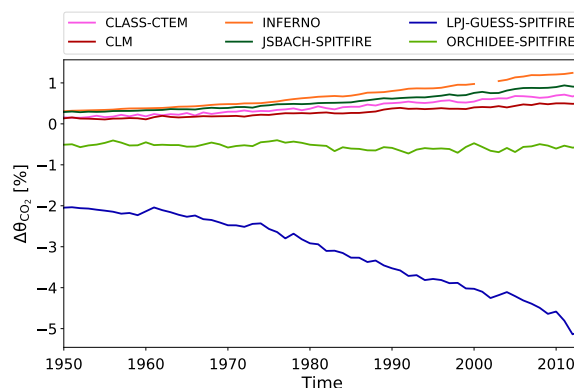


**Figure 6.** Annual average of the relative difference in volumetric soil moisture (CLM) and total soil moisture content (remaining models) between the baseline experiment SF1 and the sensitivity experiment SF2\_CO2 (see tab. 1;  $\Delta\theta_{\text{CO}_2}$ ) for 1950–2013 in %. Due to a postprocessing error, INFERNO lacks two years (2002 and 2003).

The higher vegetation biomass shown by all models is expected as studies showed that elevated  $\text{CO}_2$  increases the productivity (Farquhar et al., 1980; Hickler et al., 2008) and water-use efficiency (De Kauwe et al., 2013). Increased productivity and vegetation storage leads to higher and faster fuel build-up. The higher water-use efficiency can decrease flammability through increased soil moisture. Additionally an increase in woody plants is expected (Wigley et al., 2010; Buitenwerf et al., 2012; Bond and Midgley, 2012), which have coarser and less flammable fuel. Decreases in flammability lead to reduced burned area. The strength of  $\text{CO}_2$  effects on productivity and allocation is still uncertain. Comparisons with experimental data suggest that models that do not include the nitrogen cycle overestimate the effect on productivity (Hickler et al., 2015). However, an analysis using an observation-based emergent constraint on the longterm sensitivity of land carbon storage shows that models from the Coupled Climate Model Intercomparison Project (CMIP5) ensemble that included an interactive nitrogen cycle underestimate the impact of  $\text{CO}_2$  on productivity (Wenzel et al., 2016).

### 3.2.2 Sensitivity of models to population density

The population density forcing used for FireMIP increases in every region of the globe over time as well as in annual global values (Goldewijk et al., 2010). This increasing population density is associated with a monotonic increase of global burned area for LPJ-GUESS-SPITFIRE, and a monotonic decrease for LPJ-GUESS-SIMFIRE-BLAZE and CLM. The remaining models show a peak in the impact of population density on burned area around 1950 and a subsequent decline (see fig. 2, b).

All the models, except LPJ-GUESS-SIMFIRE-BLAZE, include the number of anthropogenic ignitions ( $I_A$ ) or the probability of fire due to anthropogenic ignitions ( $P_{i,h}$  in CLASS-CTEM) in the calculation of burned area. Most of the models represent the number of anthropogenic ignitions with an increase up to a certain threshold number and then a decline, implicitly assuming that for high population densities humans tend to suppress fires (SPITFIRE-models, INFERNO and CLM; see fig. 7). CLASS-CTEM, JSBACH-SPITFIRE and CLM include explicit terms to account for the effects of suppression not only on



ignitions but also on fire size, or duration, or both (see fig. 8). The combination of the ignition and suppression term in CLASS-CTEM leads to a maximum impact of humans on burned area at intermediate population density. The combination of ignition and suppression mechanisms dependant on population thresholds explains why most of the models have non-monotonic changes in burned area as population increases during the 20th century. LPJ-GUESS-SPITFIRE is the only model that shows a monotonic increase in burned area in response to increasing population density; other models that include the SPITFIRE fire module (JSBACH, ORCHIDEE) show the non-monotonic trajectory that results from the shift from the dominance of ignitions to that of suppression on burned area. ORCHIDEE-SPITFIRE has a much lower contribution from anthropogenic ignitions than LPJ-GUESS-SPITFIRE and therefore different spatial patterns of burned area (see fig. A1); JSBACH-SPITFIRE has an additional suppression term. The inclusion of additional suppression mechanisms may also explain the behavior of CLM, which shows a monotonic decrease in burned area over the 20th century.

LPJ-GUESS-SIMFIRE-BLAZE does not include anthropogenic ignitions explicitly but rather treats the net effect of changes in population density, which was optimized using burned-area satellite data (Knorr et al., 2014). This optimized net effect is a monotonic decrease of burned area with increases in population density. This explains why this model shows a monotonic decrease overall and indeed is the only model that shows almost no grid cell with a positive trend in burned area (see fig. 3, A4).

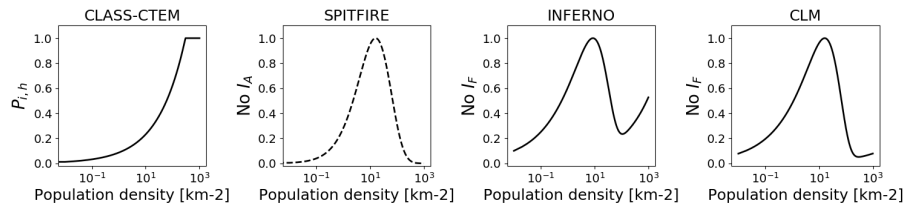


**Figure 7.** Variation in probability of fire due to human ignitions ( $P_{i,h}$ ), anthropogenic ignitions ( $No I_A$ ) or number of fires ( $No I_F$ ) for changes in population density. Since all models use different units, the values are scaled to the value range [0,1].

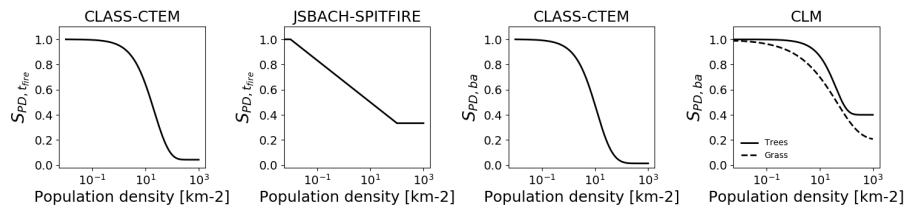


**Figure 8.** Suppressive effects of population density on fire duration ( $S_{PD,t_{fire}}$ ) for CLASS-CTEM and JSBACH SPITFIRE and suppressive effects on fire size ( $S_{PD,b_a}$ ) for CLASS-CTEM and CLM. All models are scaled to the value range [0,1].

The models all agree that for high population density fire is suppressed, but differ on their assumptions what happens for low population density and the threshold where humans start to suppress fire and whether explicit suppression is included. This leads to some similarities in the spatial patterns of the effect of population changes (see fig. A4). The net or emerging effect of



humans on burned area in models, however, also depends on the presence of lightning ignitions. As soon as lightning ignitions are present, the net effect of humans is to suppress fires, even when the underlying relationship assumes an increase in ignitions with population density (Arora and Melton, 2018, supplement). This may explain why global models assuming an increase of ignitions with increases in population density are able to capture the burned area variation along population density gradients  
 5 (Lasslop and Kloster, 2017; Arora and Melton, 2018) although global statistical analysis support a net human suppression also for low population density (Bistinas et al., 2014).

### 3.2.3 Sensitivity of models to land-use change

The land-use change imposed in SF2\_FLA over the recent centuries is characterized by a strong decrease in forested areas, and an increase in pastures and croplands (Hurt et al., 2011). The FireMIP-models do not show a uniform response of burned area  
 10 to land-use change. LPJ-GUESS-SPITFIRE shows the strongest reaction with a monotonic increase in burned area with land-use change. INFERNO and ORCHIDEE-SPITFIRE also show an increasing trend, but of lower magnitude. CLASS-CTEM, JSBACH-SPITFIRE and LPJ-GUESS-SIMFIRE-BLAZE show a decreased burned area due to increased land-use. CLM also shows a decrease in burned area but this change is comparatively muted (see fig. 2, c)).

The FireMIP-models handle land-cover dynamics, the expansion of agricultural areas and fire in agricultural areas differently.  
 15 Some of the models (CLASS-CTEM, CLM, JSBACH-SPITFIRE, ORCHIDEE-SPITFIRE) prescribe the vegetation distribution, so that the land cover fraction for all PFTs does not change through time in SF2\_FLA while in the SF1 simulation the cover fractions of natural PFTs are reduced according to the expansion of agricultural areas. The other models simulate the distribution of the natural vegetation dynamically, but prescribe the agricultural areas. All models decrease the tree cover to represent the expansion of croplands over time. Land conversion due to the expansion of pasture is not represented in CLASS-  
 20 CTEM. Only CLM includes cropland fires, INFERNO treats croplands as natural grasslands and all the other models exclude croplands from burning (see tab. 5). Therefore for all models except CLM and INFERNO, increases in cropland area lead to a reduction in burned area and the reasons for the divergence of the other models must be caused by the treatment of pastures.

**Table 5.** Treatment of agricultural fires (Rabin et al., 2017b). 'None' indicates the vegetation type does not burn or that deforestation fires are not represented in the model. The models treating pasture fire the same as grassland do not treat pasture as a specific PFT. The indication 'no pasture' means that there is no land cover change due to pastures.

Model	Cropland fire	Pasture fire	Deforestation fire
CLASS-CTEM	None	no pasture	None
CLM	Yes	Same as grassland	Yes
INFERNO	Same as grasslands	Same as grassland	None
JSBACH-SPITFIRE	None	Higher fuel bulk density than grasslands	None
LPJ-GUESS-SIMFIRE-BLAZE	None	Harvest of biomass	None
LPJ-GUESS-SPITFIRE	None	Same as grassland	None
ORCHIDEE-SPITFIRE	None	Same as grassland	None



In LPJ-GUESS-SIMFIRE-BLAZE pastures are harvested; this reduction in biomass leads to a decrease in burned area in addition to the decrease caused by exclusion of fire in croplands. In JSBACH-SPITFIRE, the expansion of pastures occurs preferentially at the expense of natural grassland and does not affect tree cover until all the natural grassland has been replaced (Reick et al., 2013). This assumption decreases the effect of land cover conversion on tree cover. Additionally in JSBACH-  
5 SPITFIRE the fuel bulk density of pastures is higher than that of natural grass by a factor of two, which decreases fire spread and thus burned area (Rabin et al., 2017b). This difference reduces burned area in pastures compared to natural grassland. In CLASS-CTEM, which also shows a decline, pastures are not included, the only land conversion is due to the expansion of croplands.

LPJ-GUESS-SPITFIRE and ORCHIDEE-SPITFIRE react with an increase in burned area to the expansion of land-use  
10 since they treat pastures as natural grasslands. The SPITFIRE fire module is very sensitive to the vegetation type with very high burned area for natural grasslands due to higher flammability compared to woody PFTs (Lasslop et al., 2014, 2016). Fuel bulk density is an important parameter but additionally grass fuels dry out faster leading to an increase in flammability and therefore burned area if forested areas are converted to grasslands. LPJ-GUESS-SPITFIRE computes the vegetation cover dynamically, so that an increase in burned area reduces the cover fraction of woody types, which might explain the stronger  
15 response compared to ORCHIDEE-SPITFIRE. In CLM pastures are represented by increased grass cover. The biomass scaling function does not distinguish fuel types (see fig. 5), therefore the lower fuel amount of grasslands could lead to a decrease in fire probability, while the maximum fire spread rate depends on the vegetation type and is higher for grasslands (Rabin et al., 2017b). The inclusion of cropland and deforestation fires dampen the effect of land-cover change on global burned area. In INFERNO, agricultural regions are not defined explicitly. Instead, woody PFT types are excluded on agricultural area (Clark  
20 et al., 2011). INFERNO includes an average burned area for each PFT in the calculation of the burned area per PFT which leads directly to increasing grass cover resulting in higher burned area (Mangeon et al., 2016; Rabin et al., 2017b). Land-use was already identified as a main reason for inter-model spread in the CMIP5 ensemble (Kloster and Lasslop, 2017). We have shown that this largely reflects the way pastures are treated, as most models used here (except CLM and INFERNO) simply exclude croplands from burning.

#### 25 3.2.4 Sensitivity of models to lightning

Most of the models show a low sensitivity of burning rates to lightning (see fig. 2), although lightning rates increase by 20% over the simulation period. ORCHIDEE-SPITFIRE shows an increase in burned area between 1940–1960 and towards the end of the simulation. The reason can most reasonably be found in comparison to the other SPITFIRE-models and seems to be related to two points. Firstly, it uses a 12 times higher factor to convert lightning strikes to actual ignitions and anthropogenic  
30 ignitions that are 100 times lower than for the other models. Therefore, the partitioning of natural and anthropogenic ignitions is different from other SPITFIRE models (see Rabin et al., 2017b). Secondly, although a partitioning factor (SGFED) varies regionally, the per-capita ignition frequency is constant; in JSBACH-SPITFIRE and LPJ-GUESS-SPITFIRE, the per-capita ignition frequency varies regionally. This results in strong differences in the spatial patterns of burned area (see fig. A1). In consequence the strength of regions contributing to the global burned area varies between the models; ORCHIDEE-SPITFIRE



shows much more burning in the tropical and far less burning in the temperate region. Our results show that even a substantial increase (20%) in lightning has little influence on global burned area. However, lightning is known to be an important cause of ignitions regionally and is potentially involved in more complex interactions between fire, vegetation and climate, which can speed up the northward expansion of trees to the north in boreal regions (Veraverbeke et al., 2017). Thus, although we have shown that the influence of increasing lightning is negligible at a global scale, it is a potentially important factor for regional impacts.

### 3.2.5 Sensitivity of models to climate

Simulated burned area in FireMIP responds to changes in climate with strong interannual variability but only weak trends in burned area (see fig. 2, e). Only three models show a statistically significant trend in the global burned area according to a Mann-Kendall test (CLM, LPJ-GUESS-SIMFIRE-BLAZE, ORCHIDEE-SPITFIRE; see tab. 4). However, in all models the area showing an increased burned area in response to climate is higher (see fig. 3). Agreement in spatial patterns of trends between the models is however low (see fig. A7).

The influence of climate on burned area is complex; it influences burned area through the meteorological conditions and through effects on fuel load and fuel characteristics (Scott et al., 2014). We therefore correlated for each grid cell changes in physical parameters (precipitation, temperature and soil moisture) and vegetation parameters (litter, vegetation carbon and grass biomass) with changes in burned area. We find that the correlation between the individual parameters and burned area is low (see fig. A8). The absolute rank correlations are lower at the monthly scale than at the annual scale. However, at the monthly scale the number of grid cells showing significant correlations with physical parameters is higher than the number showing significant correlations with vegetation parameters, indicating that changes in physical parameters have more influence at shorter time scales than changes in vegetation parameters. This difference disappears with the aggregation to annual time scale. On the annual time scale, however, the mean absolute rank correlation is slightly higher for the vegetation parameters. Soil moisture which is also influenced by vegetation has a slightly higher correlation compared to precipitation and temperature too. This indicates that vegetation parameters are more influential on the longer annual time step and physical parameters on the monthly time step. The relationship between precipitation or soil moisture and burned area is expected to be negative, while the impact of temperature is expected to be positive. This is clearly reflected in the percentage of positively significant correlations at the annual scale, but is less clear at the monthly time step. This might reflect that the seasonality of temperature, precipitation and vegetation parameter is often synchronized and therefore the effects of the parameters cannot be separated. The low correlation between individual parameters and burned area reflects the complex interactions between the climatic drivers, vegetation conditions and fire weather.

The impact of climate on the interannual variability is, however, strongly expressed in the simulated burned area. This is consistent with the finding that recent precipitation changes influence interannual variability in fire but have little impact on recent longer-term trends (Andela et al., 2017). To fully understand the impact of the changes in climate, a number of simulations would be necessary, where only individual climate parameters change while the others are kept constant. In addition, simulations where combinations of variables change, might give further insights on the synergies between the variables. An



alternative approach, given the complex interactions between climate variables, might be to disentangle the model signals using multivariate analyses (see e.g. Forkel et al., 2019).

### 3.3 Implications for model development and applications

The huge spread of simulated burned area trends for any of the forcing factors indicates the high uncertainties in burned area trajectories. With the current state of knowledge, the use of a model ensemble that covers the model structural uncertainties is clearly the best approach for projections. Nevertheless, our analyses suggest a number of promising avenues for further model development and indicates which analysis of observational data would be useful to constrain global models. Improvements of global models will be particularly important to improve the future projections of fire-enabled models to support land management strategies for instance in the context of climate change mitigation.

Representing human influence on fire is the major challenge for long-term projections. Our analyses of the controls on the variability of fire suggest that human activities drive the long term (decadal to centennial) trajectories, while considering climate variability may be sufficient for short-term projections. The large divergence in the response to human activities between the FireMIP models shows that the human impact on fires is still insufficiently understood and therefore poorly represented in current models. There is strong inter-model agreement that burned area is suppressed at high population densities, which means that most models show a similar spatial distribution of fire-prone areas (see fig. A4) and a reduction of the burned area in the last decades of the simulation due to increases in population density. However, the reduction in global burned area in the reference simulation is for most models still much smaller than shown by satellite observations (Andela et al., 2017). This could be solved by increasing the suppression effect of humans through population density in the models, however, it could also be related to land-use and for LPJ-GUESS-SPITFIRE and JSBACH-SPITFIRE to overestimation of the CO<sub>2</sub> fertilization effect. The level of socioeconomic development also modifies the relationship between population density and burned area (Andela et al., 2017; Forkel et al., 2017); further analyses are required to better disentangle the balance of the different driving factors.

We have identified land-use change as the major cause of inter-model spread. Only one model included fires associated with land use and land cover change (cropland and deforestation fires), all the other models only included such effects through changes in vegetation parameters and structure. Croplands are simply excluded from burning in all but one model. The spread of the other models is therefore likely related to the treatment of pastures. The inclusion of cropland fires is certainly important to understand and predict changes in emissions, air pollution and the carbon cycle (Li et al., 2018). Cropland fires are due to their small extent and low intensity still a major uncertainty in remote sensing datasets (Randerson et al., 2012). High resolution remote sensing may help to improve the detection. But increased understanding in regional differences why and when people burn croplands may help to find an adequate representation of cropland fires within models. Pastures contribute over 40% of the global burned area (Rabin et al., 2015). Pasture fires are not treated explicitly in any of the models, although some models slightly modify the vegetation on pastures, by harvesting or changing the fuel bulk density (see 5). Since most models implement expansion of pastures simply by increasing the area of grasslands, information on how fuel properties differ between pastures and natural grasslands could help to improve model parametrisations. Grazing intensity was found to be related



to decreases in burned area (Andela et al., 2017). It therefore may be necessary to include information on grazing intensity, or better information on pasture management in general, to represent pastures realistically within global fire models.

In contrast to many model simulations that use a lightning climatology based on satellite observations, the FireMIP experiments were driven by a transient dataset of lightning activity created by scaling a mean monthly climatology of lightning activity using convective available potential energy (CAPE) anomalies. Although we do not detect large signals in global burned area due to changes in lightning, the impact of changes in lightning at a regional scale (and particularly in boreal regions) is considerable. Since climate changes can be expected to cause changes in lightning, it will be important to develop transient lightning datasets for climate change studies on fire. Using present day lightning patterns, for example, will certainly lead to an overestimation of lightning strikes in regions with drier climate projected in the future. The covariation with climate as well as the temporal resolution are important (Felsberg et al., 2018). The FireMIP dataset was developed using only a limited amount of information about the covariation of precipitation, CAPE and lightning; further analyses of these relationships would be useful.

It is obvious that remotely sensed burned area datasets alone are not a sufficient basis to evaluate fire models as many model structures can lead to reasonable burned area patterns. It is important to test how well current models represent the number of fires, the size of individual fires and fire intensity. Both the effects of fire on vegetation (combustion of biomass and tree mortality; Williams et al., 1999; Wooster et al., 2005) and of plume heights for fire emissions to the atmosphere (Veira et al., 2016) are a function of fire intensity. The emergence of longer records of burned area and the increasing availability of information on other aspects of the fire regime should considerably improve opportunities to evaluate and improve our models. The FRY database (Laurent et al., 2018) and the global fire atlas (Andela et al., 2018), for example provide information on fire size, numbers of fire, and the characteristics of fire patches. Exploiting such datasets should help to constrain the internal mechanisms of fire models and hopefully allow to improve the balance of different drivers.

#### 4 Summary and conclusions

The analysis presented here improves our understanding of global modelling of burned area and uncertainties associated with specific drivers and process representations in the models. The identified differences in fire models also provide information to focus analysis of observations that aim to provide constraints for global fire models. Although burned area in most models compares reasonably well with satellite observations, there is a huge spread in transient simulations before the satellite era and a huge spread in the influence of the driving factors between models.

The analysis of the sensitivity experiments showed that: (1) The increase in atmospheric CO<sub>2</sub> concentration over the 20th century leads to increased burned area in regions where fuel loads increase, but to decreased burned area in regions where tree density or coarse fuels with lower flammability increase or increases in soil moisture decrease flammability. Although models agree that the available fuel increases, the type of fuel and vegetation composition are, however, critical to understand the influence of CO<sub>2</sub> on simulated burned area.

(2) Most models link the number of ignitions to population in a way that ignitions increase initially at low population densities.



In densely populated regions, all models assume that the effect of anthropogenic ignitions is outweighed by fire suppression and the increased fragmentation of the landscape by anthropogenic land use. Whether the model shows an overall increase, a decrease or an initial increase followed by a decrease in burned area over the 20th century depends largely on the population threshold assumed for the transition from increasing ignitions to increasing suppression, and the complexity of the treatment of fire suppression.

(3) The simulated response of burned area to land-use and land cover change depends on how fires in cropland and pastureland are treated in each model. Most models simply exclude croplands from the burnable area, therefore the treatment of pastures contributes the largest part of the model spread. Models that do not allow fire in croplands, and either harvest biomass in pastures or assume specific vegetation parameters, show a reduction in burned area. Models that treat pastures as natural grasslands and distinguish different fuel types or strongly increase burned area for grasslands show an increase in burned area.

(4) The models are comparatively insensitive to changes in lightning, likely because lightning ignitions are not a limiting factor in many regions with very high burning. Previous studies however show the importance of lightning and changes in lightning for burned area in the boreal region. Therefore especially regional studies should pay attention to this factor.

(5) None of the models shows a strong trend due to changing climate but all of them show a strong influence on the interannual variability. Climatic and ecosystem parameters are only able to explain a rather small part of this variation, with stronger correlations for the ecosystem parameters on the longer annual time scale and stronger relationship with climatic parameters on the monthly time scale.

Different drivers of burned area affect different time scales: the anthropogenic factors influence long term variability, while climate, and lightning affect short-term variability. Understanding the influence of climate and lightning is especially important for interannual variability and extreme events. On the other hand understanding the impact of anthropogenic drivers are likely more important for the longer term changes of fire as for instance needed, for instance, in Earth system models.

The uncertainties in global fire models need to be taken into account in model applications, for instance if model simulations are to be used to design climate adaptation strategies. Using model ensembles can be suitable to provide estimates of the uncertainties.

25 *Code availability.*

*Data availability.* Datasets will be available after acceptance of the paper

*Code and data availability.*



Sample availability.

## Appendix A

### A1

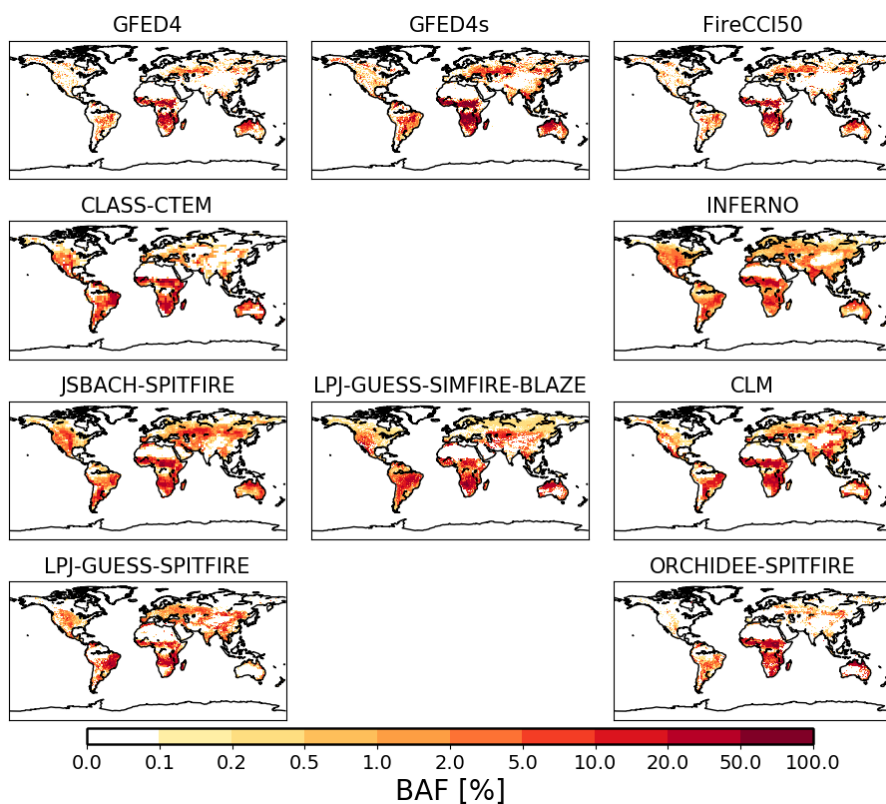


**Figure A1.** Spatial distribution annual burned area fraction (BAF) of a grid cell in % for the baseline experiment SF1 and observation data, averaged over 2001-2013.

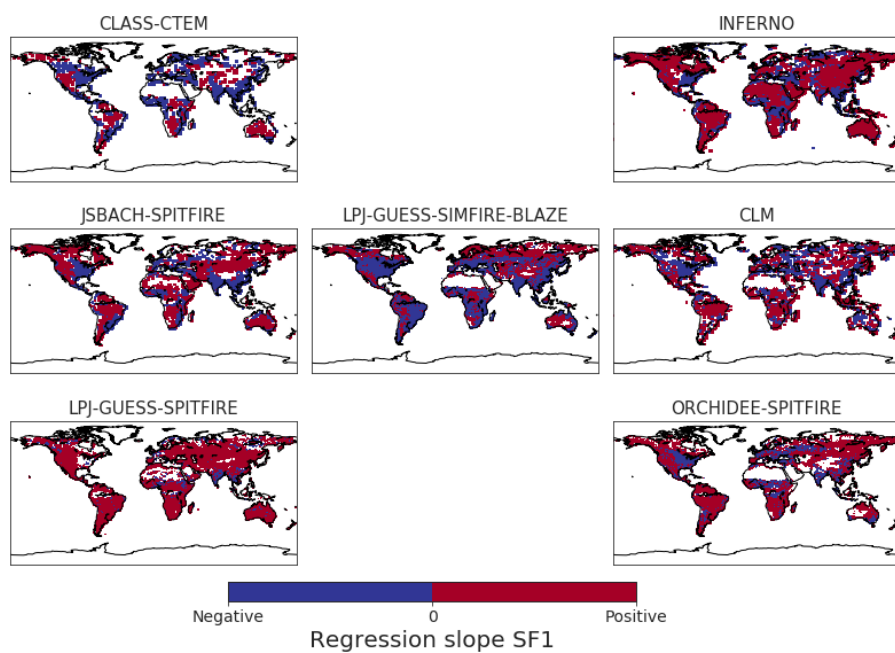


**Figure A2.** Regression slope of a grid cell for the baseline experiment SF1 over 1901-2013.

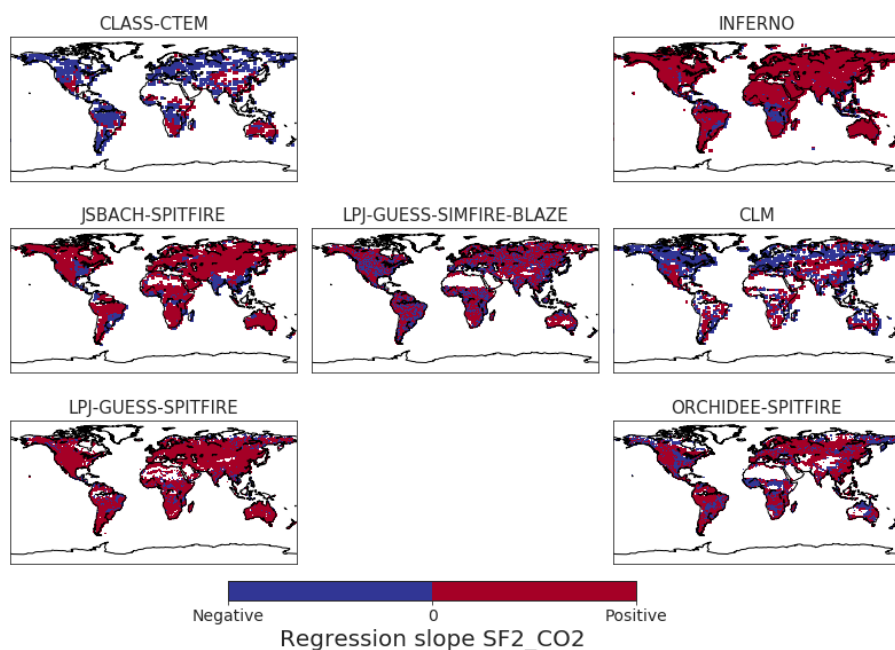


**Figure A3.** Regression slope of a grid cell for the difference between the baseline experiment SF1 and the sensitivity experiment SF2\_CO2 (SF1-SF2\_CO2; see tab. 1) over 1901-2013.

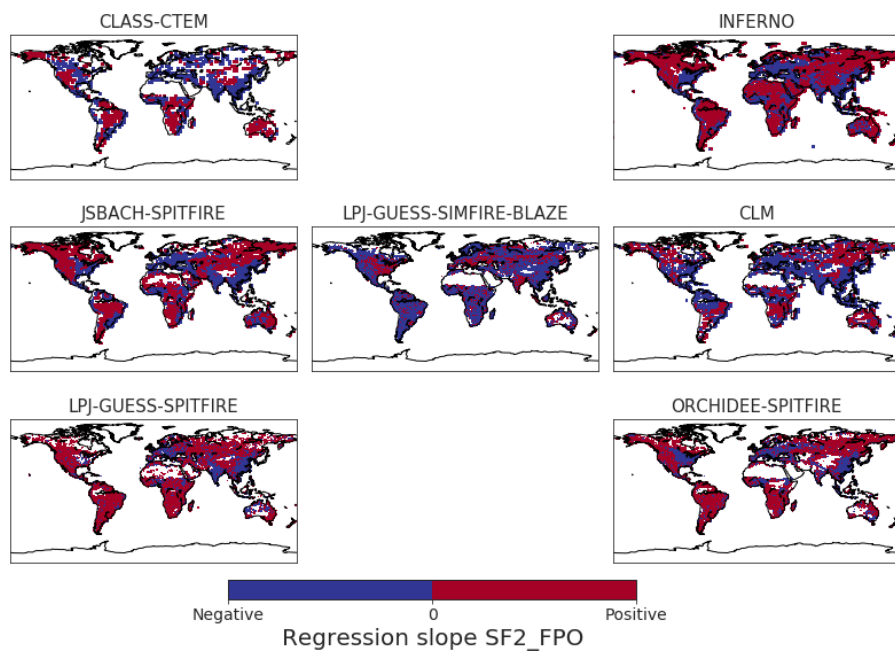


**Figure A4.** Regression slope of a grid cell for the difference between the baseline experiment SF1 and the sensitivity experiment SF2\_FPO (SF1–SF2\_FPO; see tab. 1) over 1901-2013.

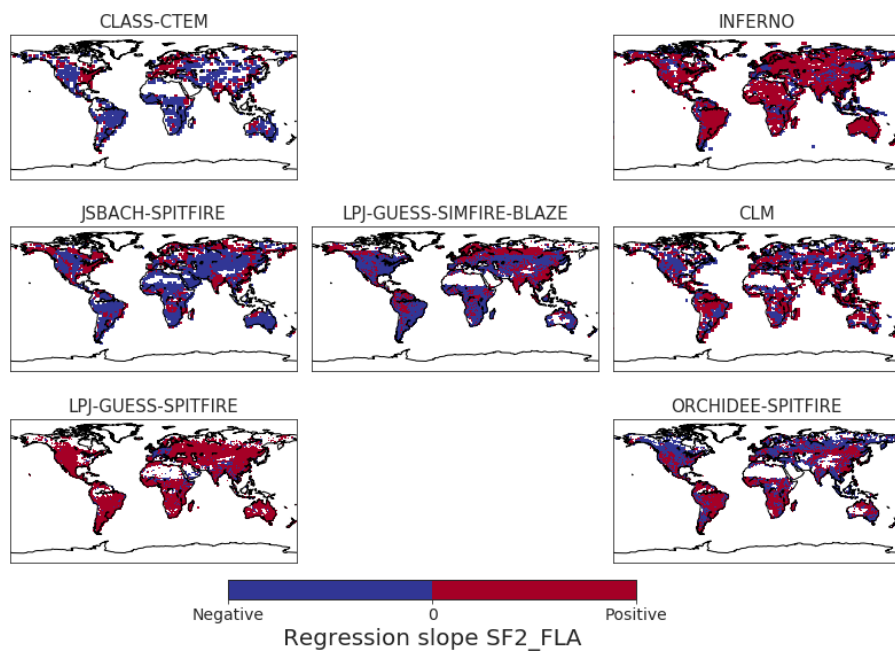


**Figure A5.** Regression slope of a grid cell for the difference between the baseline experiment SF1 and the sensitivity experiment SF2\_FLA (SF1–SF2\_FLA; see tab. 1) over 1901-2013.

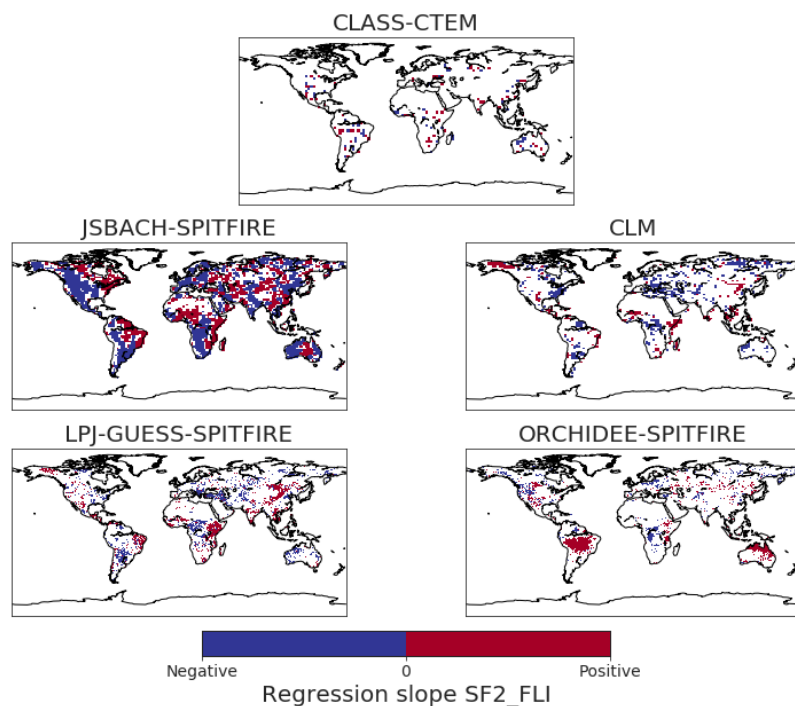


**Figure A6.** Regression slope of a grid cell for the difference between the baseline experiment SF1 and the sensitivity experiment SF2\_FLI (SF1-SF2\_FLI; see tab. 1) over 1901-2013.

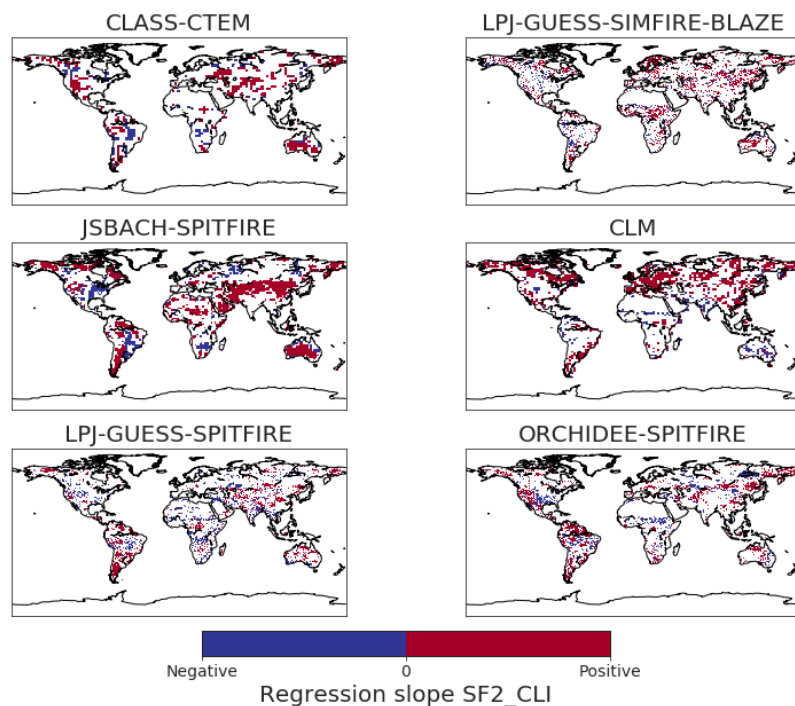


**Figure A7.** Regression slope of a grid cell for the difference between the baseline experiment SF1 and the sensitivity experiment SF2\_CLI (SF1-SF2\_CLI; see tab. 1) over 1901-2013.

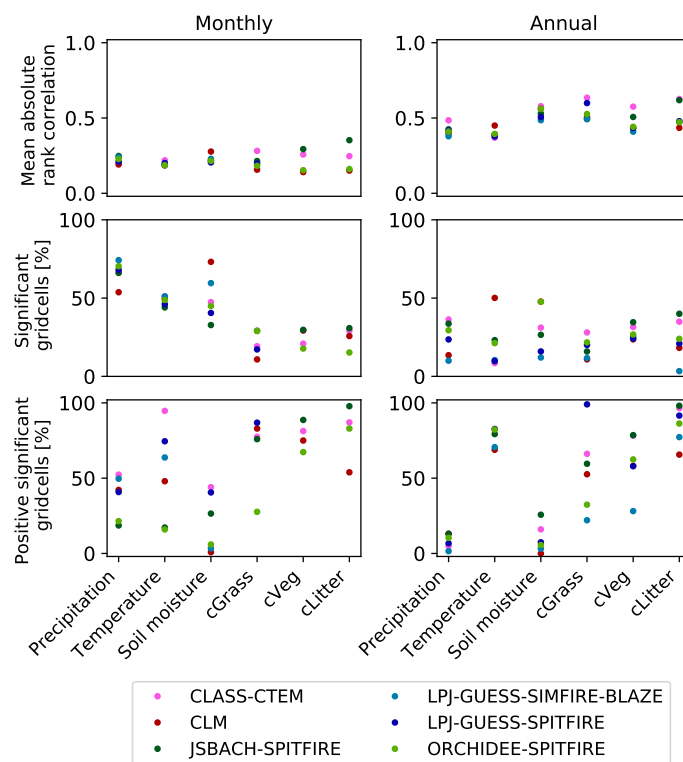


**Figure A8.** Spearman rank-order correlation coefficient for each grid cell over 1901–2013 between the relative difference between the baseline experiment SF1 and the sensitivity experiment SF2\_CLI (see tab. 1) for annual burned area fraction and precipitation, temperature, carbon stored in litter, carbon stored in vegetation, carbon stored in grass and in soil moisture, respectively. The upper panel shows the mean absolute rank correlation, i.e. the spatial average over the absolute and significant Spearman rank-order correlation coefficients where the relative difference in burned area fraction is  $> 0.1$ . The second panel shows the proportion of grid cells with a significant correlation. The lowest panels indicate the percentage of significant grid cells with a positive correlation.

**Table A1.** Reference literature for FireMIP models.

Model	Land/ Vegetation model	Fire model
CLASS-CTEM	Arora and Boer (2005)	Arora and Boer (2005)
	Melton and Arora (2016)	Melton and Arora (2016)
CLM	Oleson et al. (2013)	Li et al. (2012, 2013, 2014)
INFERNO	J. Best et al. (2011), Clark et al. (2011)	Mangeon et al. (2016)
JSBACH-SPITFIRE	Reick et al. (2013)	Lasslop et al. (2014)
		Hantson et al. (2015a)
LPJ-GUESS-SIMFIRE-BLAZE	Smith et al. (2001, 2014)	Knorr et al. (2016)
	Lindeskog et al. (2013)	
LPJ-GUESS-SPITFIRE	Smith et al. (2001)	Lehsten et al. (2009, 2015)
	Sitch et al. (2003)	
	Ahlström et al. (2012)	
ORCHIDEE-SPITFIRE	Krinner et al. (2005)	Yue et al. (2014, 2015)

**Table A2.** Correlation coefficients between burned area simulated by the FireMIP-models within the baseline experiment SF1 and the respective observation data. Due to the very skewed distribution of burned area, we use a square root transformation on both model and observations. Numbers in brackets show the Pearson correlation coefficients for not-transformed data. GFED4 and FireCCI50 provide uncertainty estimates. Correlation coefficients for 33% show the correlation between all grid points that lie within the 0–33% percentile of the relative standard error; values for 66% lie within the 33–66% percentile of the relative standard error and values for 99% lie within the 66–99% percentile. Bold numbers indicate correlation coefficients that are significant ( $p$ -value < 0.001).

Model	GFED4			FireCCI50		
	33%	66%	99%	33%	66%	99%
CLASS-CTEM	<b>0.59 (0.41)</b>	-0.08 (-0.07)	0.04 (-0.03)	<b>0.58 (0.38)</b>	-0.02 (-0.04)	0.06 (0.003)
CLM	<b>0.78 (0.72)</b>	0.13 (0.14)	0.09 (-0.03)	<b>0.80 (0.73)</b>	0.11 (0.10)	0.09 (-0.03)
INFERNO	<b>0.76 (0.68)</b>	<b>-0.18 (-0.13)</b>	0.05 (-0.02)	<b>0.77 (0.64)</b>	-0.01 (0.01)	0.05 (0.03)
JSBACH-SPITFIRE	<b>0.69 (0.62)</b>	-0.08 (-0.11)	0.02 (-0.05)	<b>0.68 (0.56)</b>	-0.01 (-0.04)	0.06 (0.01)
LPJ-GUESS-SIMFIRE-BLAZE	<b>0.70 (0.55)</b>	-0.06 (-0.07)	-0.05 (-0.10)	<b>0.67 (0.48)</b>	0.03 (0.04)	-0.04 (-0.08)
LPJ-GUESS-SPITFIRE	<b>0.56 (0.46)</b>	<b>0.42 (0.41)</b>	<b>0.31 (0.17)</b>	<b>0.61 (0.48)</b>	<b>0.40 (0.33)</b>	<b>0.47 (0.34)</b>
ORCHIDEE-SPITFIRE	<b>0.82 (0.74)</b>	<b>0.51 (0.35)</b>	<b>0.48 (0.36)</b>	<b>0.81 (0.74)</b>	<b>0.49 (0.31)</b>	<b>0.47 (0.30)</b>

*Author contributions.* LT and GL designed the study and performed the analysis with input from SPH, AH and SH. GL, SH, MF, LF, CY, JM provided simulations. LT wrote the manuscript with contributions from all authors.



*Competing interests.*

*Disclaimer.*

*Acknowledgements.* GL acknowledges the excellent computing support of DKRZ.



## References

- Ahlström, A., Schurgers, G., Arneth, A., and Smith, B.: Robustness and uncertainty in terrestrial ecosystem carbon response to CMIP5 climate change projections, *Environmental Research Letters*, 7, 044008, <https://doi.org/10.1088/1748-9326/7/4/044008>, <https://doi.org/10.1088%2F1748-9326%2F7%2F4%2F044008>, 2012.
- 5 Andela, N. and van der Werf, G. R.: Recent trends in African fires driven by cropland expansion and El Niño to La Niña transition, *Nature Climate Change*, 4, 791, <https://doi.org/http://dx.doi.org/10.1038/nclimate2313>, <https://www.nature.com/articles/nclimate2313#supplementary-information>, 2014.
- Andela, N., Morton, D. C., Giglio, L., Chen, Y., van der Werf, G. R., Kasibhatla, P. S., DeFries, R. S., Collatz, G. J., Hantson, S., Kloster, S., Bachelet, D., Forrest, M., Lasslop, G., Li, F., Mangeon, S., Melton, J. R., Yue, C., and Randerson, J. T.: A human-driven decline in  
10 global burned area, *Science*, 356, 1356–1362, <https://doi.org/10.1126/science.aal4108>, <http://science.sciencemag.org/content/356/6345/1356>, 2017.
- Andela, N., Morton, D. C., Giglio, L., Paugam, R., Chen, Y., Hantson, S., van der Werf, G. R., and Randerson, J. T.: The Global Fire Atlas of individual fire size, duration, speed, and direction, *Earth System Science Data Discussions*, pp. 1–28, <https://doi.org/10.5194/essd-2018-89>, <https://www.earth-syst-sci-data-discuss.net/essd-2018-89/>, 2018.
- 15 Archibald, S., Scholes, R. J., Roy, D. P., Roberts, G., and Boschetti, L.: Southern African fire regimes as revealed by remote sensing, *International Journal of Wildland Fire*, 19, 861–878, <https://doi.org/https://doi.org/10.1071/WF10008>, 2010.
- Arora, V. K. and Boer, G. J.: Fire as an interactive component of dynamic vegetation models, *Journal of Geophysical Research: Biogeosciences*, 110, <https://doi.org/10.1029/2005JG000042>, <https://agupubs.onlinelibrary.wiley.com/doi/abs/10.1029/2005JG000042>, 2005.
- Arora, V. K. and Melton, J. R.: Reduction in global area burned and wildfire emissions since 1930s enhances carbon uptake by land, *Nature  
20 Communications*, 9, 1326, <https://doi.org/10.1038/s41467-018-03838-0>, <http://www.nature.com/articles/s41467-018-03838-0>, 2018.
- Balch, J. K., Bradley, B. A., Abatzoglou, J. T., Nagy, R. C., Fusco, E. J., and Mahood, A. L.: Human-started wildfires expand the fire niche across the United States, *Proceedings of the National Academy of Sciences*, 114, 2946–2951, <https://doi.org/10.1073/pnas.1617394114>, <http://www.pnas.org/lookup/doi/10.1073/pnas.1617394114>, 2017.
- Bistinas, I., Harrison, S. P., Prentice, I. C., and Pereira, J. M. C.: Causal relationships versus emergent patterns in the global controls of  
25 fire frequency, *Biogeosciences*, 11, 5087–5101, <https://doi.org/10.5194/bg-11-5087-2014>, <http://www.biogeosciences.net/11/5087/2014/>, 2014.
- Bond, W. J. and Midgley, G. F.: Carbon dioxide and the uneasy interactions of trees and savannah grasses, *Philosophical Transactions of the Royal Society B: Biological Sciences*, 367, 601–612, <http://www.ncbi.nlm.nih.gov/pmc/articles/PMC3248705/>, 2012.
- Bond, W. J., Woodward, F. I., and Midgley, G. F.: The global distribution of ecosystems in a world without fire, *New Phytologist*, 165,  
30 525–538, <https://doi.org/10.1111/j.1469-8137.2004.01252.x>, <http://dx.doi.org/10.1111/j.1469-8137.2004.01252.x>, 2005.
- Bowman, D. M. J. S., Balch, J. K., Artaxo, P., Bond, W. J., Carlson, J. M., Cochrane, M. A., D’Antonio, C. M., DeFries, R. S., Doyle, J. C., Harrison, S. P., Johnston, F. H., Keeley, J. E., Krawchuk, M. A., Kull, C. A., Marston, J. B., Moritz, M. A., Prentice, I. C., Roos, C. I., Scott, A. C., Swetnam, T. W., van der Werf, G. R., and Pyne, S. J.: Fire in the Earth System, *Science*, 324, 481–484, <https://doi.org/10.1126/science.1163886>, <http://science.sciencemag.org/content/324/5926/481>, 2009.
- 35 Bowman, D. M. J. S., Balch, J., Artaxo, P., Bond, W. J., Cochrane, M. A., D’Antonio, C. M., DeFries, R., Johnston, F. H., Keeley, J. E., Krawchuk, M. A., Kull, C. A., Mack, M., Moritz, M. A., Pyne, S., Roos, C. I., Scott, A. C., Sodhi, N. S., and Swetnam, T. W.: The



- human dimension of fire regimes on Earth, *Journal of Biogeography*, 38, 2223–2236, <https://doi.org/10.1111/j.1365-2699.2011.02595.x>, <http://dx.doi.org/10.1111/j.1365-2699.2011.02595.x>, 2011.
- Buitenwerf, R., Bond, W. J., Stevens, N., and Trollope, W. S. W.: Increased tree densities in South African savannas: >50 years of data suggests CO<sub>2</sub> as a driver, *Global Change Biology*, 18, 675–684, <https://doi.org/10.1111/j.1365-2486.2011.02561.x>, <http://dx.doi.org/10.1111/j.1365-2486.2011.02561.x>, 2012.
- Chapin, F. S., Matson, P. A., and Mooney, H. A.: *Principles of Terrestrial Ecosystem Ecology*, Springer, 2002.
- Chuvieco, E., Giglio, L., and Justice, C.: Global characterization of fire activity: Toward defining fire regimes from Earth observation data, *Global Change Biology*, 14, 1488 – 1502, 2008.
- Chuvieco, E., Lizundia-Loiola, J., Pettinari, M. L., Ramo, R., Padilla, M., Tansey, K., Mouillot, F., Laurent, P., Storm, T., Heil, A., and Plummer, S.: Generation and analysis of a new global burned area product based on MODIS 250 m reflectance bands and thermal anomalies, *Earth System Science Data*, pp. 2015–2031, <https://doi.org/10.5194/essd-10-2015-2018>, <https://www.earth-syst-sci-data.net/10/2015/2018/>, 2018.
- Clark, D. B., Mercado, L. M., Sitch, S., Jones, C. D., Gedney, N., Best, M. J., Pryor, M., Rooney, G. G., Essery, R. L. H., Blyth, E., Boucher, O., Harding, R. J., Huntingford, C., and Cox, P. M.: The Joint UK Land Environment Simulator (JULES), model description – Part 2: Carbon fluxes and vegetation dynamics, *Geoscientific Model Development*, 4, 701–722, <https://doi.org/10.5194/gmd-4-701-2011>, <https://www.geosci-model-dev.net/4/701/2011/>, 2011.
- Conklin, H. C.: The Study of Shifting Cultivation, *Current Anthropology*, 2, 27–61, <http://www.jstor.org/stable/2739597>, 1961.
- De Kauwe, M. G., Medlyn, B. E., Zaehle, S., Walker, A. P., Dietze, M. C., Hickler, T., Jain, A. K., Luo, Y., Parton, W. J., Prentice, I. C., Smith, B., Thornton, P. E., Wang, S., Wang, Y.-P., Wårlind, D., Weng, E., Crous, K. Y., Ellsworth, D. S., Hanson, P. J., Seok Kim, H., Warren, J. M., Oren, R., and Norby, R. J.: Forest water use and water use efficiency at elevated CO<sub>2</sub>: a model-data intercomparison at two contrasting temperate forest FACE sites, *Global Change Biology*, 19, 1759–1779, <https://doi.org/10.1111/gcb.12164>, <http://doi.wiley.com/10.1111/gcb.12164>, 2013.
- Dumond, D. E.: Swidden Agriculture and the Rise of Maya Civilization, *Southwestern Journal of Anthropology*, 17, 301–316, <https://doi.org/10.1086/soutjanth.17.4.3628942>, <https://doi.org/10.1086/soutjanth.17.4.3628942>, 1961.
- Ehleringer, J. and Björkman, O.: Quantum Yields for CO<sub>2</sub> Uptake in C<sub>3</sub> and C<sub>4</sub> Plants, *Plant Physiology*, 59, 86–90, <https://doi.org/10.1104/pp.59.1.86>, <http://www.plantphysiol.org/content/59/1/86>, 1977.
- Ehleringer, J. R., Cerling, T. E., and Helliker, B. R.: C<sub>4</sub> photosynthesis, atmospheric CO<sub>2</sub>, and climate, *Oecologia*, 112, 285–299, <https://doi.org/10.1007/s004420050311>, <https://doi.org/10.1007/s004420050311>, 1997.
- Erb, K.-H., Luyssaert, S., Meyfroidt, P., Pongratz, J., Don, A., Kloster, S., Kuemmerle, T., Fetzel, T., Fuchs, R., Herold, M., Haberl, H., Jones, C. D., Marín-Spiotta, E., McCallum, I., Robertson, E., Seufert, V., Fritz, S., Valade, A., Wiltshire, A., and Dolman, A. J.: Land management: data availability and process understanding for global change studies, *Global Change Biology*, 23, 512–533, <https://doi.org/10.1111/gcb.13443>, <http://doi.wiley.com/10.1111/gcb.13443>, 2017.
- Farquhar, G. D., von Caemmerer, S., and Berry, J. A.: A biochemical model of photosynthetic CO<sub>2</sub> assimilation in leaves of C<sub>3</sub> species, *Planta*, 149, 78–90, <https://doi.org/10.1007/BF00386231>, <https://doi.org/10.1007/BF00386231>, 1980.
- Felsberg, A., Kloster, S., Wilkenskjeld, S., Krause, A., and Lasslop, G.: Lightning Forcing in Global Fire Models: The Importance of Temporal Resolution, *Journal of Geophysical Research: Biogeosciences*, 123, <https://doi.org/10.1002/2017JG004080>, 2018.
- Finlay, S. E., Moffat, A., Gazzard, R., Baker, D., and Murray, V.: Health Impacts of Wildfires, *PLoS currents*, 4, e4f959951cce2c, 2012.



- Forkel, M., Dorigo, W., Lasslop, G., Teubner, I., Chuvieco, E., and Thonicke, K.: A data-driven approach to identify controls on global fire activity from satellite and climate observations (SOFIA V1), *Geoscientific Model Development*, 10, 4443–4476, <https://doi.org/10.5194/gmd-10-4443-2017>, <https://www.geosci-model-dev.net/10/4443/2017/>, 2017.
- Forkel, M., Andela, N., Harrison, S. P., Lasslop, G., van Marle, M., Chuvieco, E., Dorigo, W., Forrest, M., Hantson, S., Heil, A., Li, F., Melton, J., Sitch, S., Yue, C., and Arneth, A.: Emergent relationships with respect to burned area in global satellite observations and fire-enabled vegetation models, *Biogeosciences*, 16, 57–76, <https://doi.org/10.5194/bg-16-57-2019>, <https://www.biogeosciences.net/16/57/2019/>, 2019.
- Gauthier, S., Bernier, P., Boulanger, Y., Guo, J., Guindon, L., Beaudoin, A., and Boucher, D.: Vulnerability of timber supply to projected changes in fire regime in Canada's managed forests, *Canadian Journal of Forest Research*, 45, 1439–1447, <https://doi.org/10.1139/cjfr-2015-0079>, <https://doi.org/10.1139/cjfr-2015-0079>, 2015.
- Giglio, L., Randerson, J. T., and van der Werf, G. R.: Analysis of daily, monthly, and annual burned area using the fourth-generation global fire emissions database (GFED4), *Journal of Geophysical Research: Biogeosciences*, 118, 317–328, <https://doi.org/10.1002/jgrg.20042>, <http://dx.doi.org/10.1002/jgrg.20042>, 2013.
- Goldewijk, K. K., Beusen, A., and Janssen, P.: Long-term dynamic modeling of global population and built-up area in a spatially explicit way: HYDE 3.1, *The Holocene*, 20, 565–573, <https://doi.org/10.1177/0959683609356587>, <https://doi.org/10.1177/0959683609356587>, 2010.
- Hantson, S., Lasslop, G., Kloster, S., and Chuvieco, E.: Anthropogenic effects on global mean fire size, *International Journal of Wildland Fire*, 24, 589–596, 2015a.
- Hantson, S., Pueyo, S., and Chuvieco, E.: Global fire size distribution is driven by human impact and climate, *Global Ecology and Biogeography*, 24, 77–86, <https://doi.org/10.1111/geb.12246>, 2015b.
- Hantson, S., Arneth, A., Harrison, S. P., Kelley, D. I., Prentice, I. C., Rabin, S. S., Archibald, S., Mouillot, F., Arnold, S. R., Artaxo, P., Bachelet, D., Ciais, P., Forrest, M., Friedlingstein, P., Hickler, T., Kaplan, J. O., Kloster, S., Knorr, W., Lasslop, G., Li, F., Mangeon, S., Melton, J. R., Meyn, A., Sitch, S., Spessa, A., van der Werf, G. R., Voulgarakis, A., and Yue, C.: The status and challenge of global fire modelling, *Biogeosciences*, 13, 3359–3375, <https://doi.org/10.5194/bg-13-3359-2016>, <https://www.biogeosciences.net/13/3359/2016/>, 2016.
- Harrison, S., Marlon, J., and Bartlein, P.: *Fire in the Earth System*, pp. 21–48, Springer Netherlands, Dordrecht, [https://doi.org/10.1007/978-90-481-8716-4\\_3](https://doi.org/10.1007/978-90-481-8716-4_3), 2010.
- Harrison, S. P., Bartlein, P. J., Brovkin, V., Houweling, S., Kloster, S., and Prentice, I. C.: The biomass burning contribution to climate–carbon-cycle feedback, *Earth System Dynamics*, 9, 663–677, <https://doi.org/10.5194/esd-9-663-2018>, <https://www.earth-syst-dynam.net/9/663/2018/>, 2018.
- Hickler, T., Smith, B., Prentice, I. C., Mjöfors, K., Miller, P., Arneth, A., and Sykes, M. T.: CO<sub>2</sub> fertilization in temperate FACE experiments not representative of boreal and tropical forests, *Global Change Biology*, 14, 1531–1542, <https://doi.org/10.1111/j.1365-2486.2008.01598.x>, <http://dx.doi.org/10.1111/j.1365-2486.2008.01598.x>, 2008.
- Hickler, T., Rammig, A., and Werner, C.: Modelling CO<sub>2</sub> Impacts on Forest Productivity, *Curr. For. Reports*, 1, 69–80, <https://doi.org/10.1007/s40725-015-0014-8>, <http://link.springer.com/10.1007/s40725-015-0014-8>, 2015.
- Humber, M. L., Boschetti, L., Giglio, L., and Justice, C. O.: Spatial and temporal intercomparison of four global burned area products, *International Journal of Digital Earth*, 0, 1–25, <https://doi.org/10.1080/17538947.2018.1433727>, <https://doi.org/10.1080/17538947.2018.1433727>, 2018.



- Hurt, G. C., Chini, L. P., Froking, S., Betts, R. A., Feddema, J., Fischer, G., Fisk, J. P., Hibbard, K., Houghton, R. A., Janetos, A., Jones, C. D., Kindermann, G., Kinoshita, T., Klein Goldewijk, K., Riahi, K., Shevliakova, E., Smith, S., Stehfest, E., Thomson, A., Thornton, P., Vuuren, D. P., and Wang, Y. P.: Harmonization of land-use scenarios for the period 1500–2100: 600 years of global gridded annual land-use transitions, wood harvest, and resulting secondary lands, *Climatic Change*, 109, 117–161, <https://doi.org/10.1007/s10584-011-0153-2>,  
5 <http://link.springer.com/10.1007/s10584-011-0153-2>, 2011.
- J. Best, M., Pryor, M., Clark, D., G. Rooney, G., Essery, R., Menard, C., M. Edwards, J., Hendry, M., Porson, A., and Gedney, N.: The Joint UK Land Environment Simulator (JULES), model description – Part 1: Energy and water fluxes, *Geoscientific Model Development*, 4, 677–699, <https://doi.org/10.5194/gmd-4-677-2011>, 2011.
- Johnston, F., Henderson, S., Chen, Y., T Randerson, J., Marlier, M., Defries, R., Kinney, P., Bowman, D., and Brauer, M.: Estimated Global Mortality Attributable to Smoke from Landscape Fires, *Environmental health perspectives*, 120, 695–701, 2012.
- Johnston, K. J.: The intensification of pre-industrial cereal agriculture in the tropics: Boserup, cultivation lengthening, and the Classic Maya, *Journal of Anthropological Archaeology*, 22, 126–161, [https://doi.org/10.1016/S0278-4165\(03\)00013-8](https://doi.org/10.1016/S0278-4165(03)00013-8), <http://www.sciencedirect.com/science/article/pii/S0278416503000138>, 2003.
- Kelley, D. I. and Harrison, S. P.: Enhanced Australian carbon sink despite increased wildfire during the 21st century, *Environmental Research Letters*, 9, 104 015, 2014.
- 15 Kelley, D. I., Prentice, I. C., Harrison, S. P., Wang, H., Simard, M., Fisher, J., and Willis, K. O.: A comprehensive benchmarking system for evaluating global vegetation models, *Biogeosciences*, 10, 3313–3340, <https://doi.org/10.5194/bg-10-3313-2013>, <http://centaur.reading.ac.uk/35876/>, 2013.
- Kloster, S. and Lasslop, G.: Historical and future fire occurrence (1850 to 2100) simulated in CMIP5 Earth System Models, *Global and Planetary Change*, 150, 58–69, <https://doi.org/10.1016/j.gloplacha.2016.12.017>, <http://www.sciencedirect.com/science/article/pii/S0921818116303770>, 2017.
- 20 Kloster, S., Mahowald, N. M., Randerson, J. T., Thornton, P. E., Hoffman, F. M., Levis, S., Lawrence, P. J., Feddema, J. J., Oleson, K. W., and Lawrence, D. M.: Fire dynamics during the 20th century simulated by the Community Land Model, *Biogeosciences*, 7, 1877–1902, <http://www.biogeosciences.net/7/1877/2010/>, 2010.
- 25 Knorr, W., Kaminski, T., Arneth, A., and Weber, U.: Impact of human population density on fire frequency at the global scale, *Biogeosciences*, 11, 1085–1102, <https://doi.org/10.5194/bg-11-1085-2014>, <http://www.biogeosciences.net/11/1085/2014/>, 2014.
- Knorr, W., Jiang, L., and Arneth, A.: Climate, CO<sub>2</sub> and human population impacts on global wildfire emissions, *Biogeosciences*, 13, 267–282, <https://search.proquest.com/docview/1770227658?accountid=105241>, 2016.
- Korontzi, S., McCarty, J., Loboda, T., Kumar, S., and Justice, C.: Global distribution of agricultural fires in croplands from 30 3 years of Moderate Resolution Imaging Spectroradiometer (MODIS) data, *Global Biogeochemical Cycles*, 20, n/a–n/a, <https://doi.org/10.1029/2005GB002529>, <http://doi.wiley.com/10.1029/2005GB002529>, 2006.
- Krause, A., Kloster, S., Wilkenskjeld, S., and Paeth, H.: The sensitivity of global wildfires to simulated past, present, and future lightning frequency, *J. Geophys. Res. Biogeosciences*, 119, 312–322, <https://doi.org/10.1002/2013JG002502>, <http://doi.wiley.com/10.1002/2013JG002502>, 2014.
- 35 Krawchuk, M. a. and Moritz, M. a.: Constraints on global fire activity vary across a resource gradient., *Ecology*, 92, 121–132, <http://www.ncbi.nlm.nih.gov/pubmed/21560682>, 2011.



- Krinner, G., Viovy, N., de Noblet-Ducoudré, N., Ogée, J., Polcher, J., Friedlingstein, P., Ciais, P., Sitch, S., and Prentice, I. C.: A dynamic global vegetation model for studies of the coupled atmosphere-biosphere system, *Global Biogeochemical Cycles*, 19, <https://doi.org/10.1029/2003GB002199>, <https://agupubs.onlinelibrary.wiley.com/doi/abs/10.1029/2003GB002199>, 2005.
- Lasslop, G. and Kloster, S.: Human impact on wildfires varies between regions and with vegetation productivity, *Environmental Research Letters*, 12, 115 011, <http://stacks.iop.org/1748-9326/12/i=11/a=115011>, 2017.
- Lasslop, G., Thonicke, K., and Kloster, S.: SPITFIRE within the MPI Earth system model: Model development and evaluation, *Journal of Advances in Modeling Earth Systems*, 6, 740–755, 2014.
- Lasslop, G., Hantson, S., and Kloster, S.: Influence of wind speed on the global variability of burned fraction: A global fire model's perspective, *International Journal of Wildland Fire*, 24, <https://doi.org/10.1071/WF15052>, 2015.
- 10 Lasslop, G., Brovkin, V., Reick, C., Bathiany, S., and Kloster, S.: Multiple stable states of tree cover in a global land surface model due to a fire-vegetation feedback, *Geophysical Research Letters*, 43, <https://doi.org/10.1002/2016GL069365>, 2016.
- Laurent, P., Mouillot, F., Yue, C., Ciais, P., Moreno, M. V., and Nogueira, J. M. P.: FRY, a global database of fire patch functional traits derived from space-borne burned area products, *Scientific Data*, 5, 180 132, <https://doi.org/10.1038/sdata.2018.132>, <http://www.nature.com/articles/sdata2018132>, 2018.
- 15 Lehsten, V., Tansey, K., Balzter, H., Thonicke, K., Spessa, A., Weber, U., Smith, B., and Arneth, A.: Estimating carbon emissions from African wildfires, *Biogeosciences*, 6, 349–360, <https://doi.org/10.5194/bg-6-349-2009>, <https://www.biogeosciences.net/6/349/2009/>, 2009.
- Lehsten, V., Arneth, A., Spessa, A., Thonicke, K., and Moustakas, A.: The effect of fire on tree-grass coexistence in savannas: A simulation study, *International Journal of Wildland Fire*, 25, <https://doi.org/10.1071/WF14205>, 2015.
- 20 Li, F. and Lawrence, D. M.: Role of Fire in the Global Land Water Budget during the Twentieth Century due to Changing Ecosystems, *Journal of Climate*, 30, 1893–1908, <https://doi.org/10.1175/JCLI-D-16-0460.1>, <https://doi.org/10.1175/JCLI-D-16-0460.1>, 2017.
- Li, F., Zeng, X. D., and Levis, S.: A process-based fire parameterization of intermediate complexity in a Dynamic Global Vegetation Model, *Biogeosciences*, 9, 2761–2780, <https://doi.org/10.5194/bg-9-2761-2012>, <https://www.biogeosciences.net/9/2761/2012/>, 2012.
- Li, F., Levis, S., and Ward, D. S.: Quantifying the role of fire in the Earth system &ndash; Part 1: Improved global fire modeling  
25 in the Community Earth System Model (CESM1), *Biogeosciences*, 10, 2293–2314, <https://doi.org/10.5194/bg-10-2293-2013>, <https://www.biogeosciences.net/10/2293/2013/>, 2013.
- Li, F., Bond-Lamberty, B., and Levis, S.: Quantifying the role of fire in the Earth system – Part 2: Impact on the net carbon balance of global terrestrial ecosystems for the 20th century, *Biogeosciences*, 11, 1345–1360, <https://doi.org/10.5194/bg-11-1345-2014>, <https://www.biogeosciences.net/11/1345/2014/>, 2014.
- 30 Li, F., Lawrence, D. M., and Bond-Lamberty, B.: Impact of fire on global land surface air temperature and energy budget for the 20th century due to changes within ecosystems, *Environmental Research Letters*, 12, 044 014, <http://stacks.iop.org/1748-9326/12/i=4/a=044014>, 2017.
- Li, F., Lawrence, D. M., and Bond-Lamberty, B.: Human impacts on 20th century fire dynamics and implications for global carbon and water trajectories, *Global and Planetary Change*, 162, 18–27, <https://doi.org/10.1016/j.gloplacha.2018.01.002>, <https://linkinghub.elsevier.com/retrieve/pii/S0921818117303910>, 2018.
- 35 Lindeskog, M., Arneth, A., Bondeau, A., Waha, K., Seaquist, J., Olin, S., and Smith, B.: Implications of accounting for land use in simulations of ecosystem carbon cycling in Africa, *Earth System Dynamics*, 4, 385–407, <https://doi.org/10.5194/esd-4-385-2013>, <https://www.earth-syst-dynam.net/4/385/2013/>, 2013.



- Mangeon, S., Voulgarakis, A., Gilham, R., Harper, A., Sitch, S., and Folberth, G.: INFERNO: a fire and emissions scheme for the UK Met Office's Unified Model, *Geoscientific Model Development*, 9, 2685–2700, <https://doi.org/10.5194/gmd-9-2685-2016>, <https://www.geosci-model-dev.net/9/2685/2016/>, 2016.
- Marlon, J. R., Bartlein, P. J., Carcaillet, C., Gavin, D. G., Harrison, S. P., Higuera, P. E., Joos, F., Power, M. J., and Prentice, I. C.: Climate and human influences on global biomass burning over the past two millennia, *Nature Geoscience*, 1, 697, <https://doi.org/http://dx.doi.org/10.1038/ngeo313>, <https://www.nature.com/articles/ngeo313#supplementary-information>, 2008.
- Marlon, J. R., Bartlein, P. J., Daniiau, A.-L., Harrison, S. P., Maezumi, S. Y., Power, M. J., Tinner, W., and Vanni re, B.: Global biomass burning: a synthesis and review of Holocene paleofire records and their controls, *Quaternary Science Reviews*, 65, 5–25, <https://doi.org/10.1016/j.quascirev.2012.11.029>, <http://linkinghub.elsevier.com/retrieve/pii/S027379112005318>, 2013.
- Marlon, J. R., Kelly, R., Daniiau, A.-L., Vanni re, B., Power, M. J., Bartlein, P., Higuera, P., Blarquez, O., Brewer, S., Br ucher, T., Feurdean, A., Romera, G. G., Iglesias, V., Maezumi, S. Y., Magi, B., Courtney Mustaphi, C. J., and Zhihai, T.: Reconstructions of biomass burning from sediment-charcoal records to improve data–model comparisons, *Biogeosciences*, 13, 3225–3244, <https://doi.org/10.5194/bg-13-3225-2016>, <https://www.biogeosciences.net/13/3225/2016/>, 2016.
- McLeod, A.: Kendall: Kendall rank correlation and Mann-Kendall trend test, <https://CRAN.R-project.org/package=Kendall>, r package version 2.2, 2011.
- Melton, J. R. and Arora, V. K.: Competition between plant functional types in the Canadian Terrestrial Ecosystem Model (CTEM) v. 2.0, *Geoscientific Model Development*, 9, 323–361, <https://doi.org/10.5194/gmd-9-323-2016>, <https://www.geosci-model-dev.net/9/323/2016/>, 2016.
- Morison, J. I. L.: Sensitivity of stomata and water use efficiency to high CO<sub>2</sub>, *Plant, Cell and Environment*, 8, 467–474, <https://doi.org/10.1111/j.1365-3040.1985.tb01682.x>, <http://doi.wiley.com/10.1111/j.1365-3040.1985.tb01682.x>, 1985.
- Oleson, K., Lawrence, D., Bonan, G., Drewniak, B., Huang, M., Koven, C., Levis, S., Li, F., Riley, W., M. Subin, Z., C. Swenson, S., E. Thornton, P., Bozbiyik, A., Fisher, R., Heald, C., Kluzek, E., Lamarque, J.-F., Lawrence, P., Leung, L., and Yang, Z.-L.: Technical description of version 4.5 of the Community Land Model (CLM), 2013.
- Otto, J. S. and Anderson, N. E.: Slash-And-Burn Cultivation in the Highlands South: A Problem in Comparative Agricultural History, *Comparative Studies in Society and History*, 24, 131–147, <http://www.jstor.org/stable/178724>, 1982.
- Parisien, M.-A., Miller, C., Parks, S. A., DeLancey, E. R., Robinne, F.-N., and Flannigan, M. D.: The spatially varying influence of humans on fire probability in North America, *Environmental Research Letters*, 11, 075 005, <https://doi.org/10.1088/1748-9326/11/7/075005>, <http://stacks.iop.org/1748-9326/11/i=7/a=075005?key=crossref.190a89a50156e98edb97a10a80527a05>, 2016.
- Peterson, D., Wang, J., Ichoku, C., and Remer, L. A.: Effects of lightning and other meteorological factors on fire activity in the North American boreal forest: implications for fire weather forecasting, *Atmospheric Chemistry and Physics*, 10, 6873–6888, <https://doi.org/doi:10.5194/acp-10-6873-2010>, 2010.
- Pettinari, M. L. and Chuvieco, E.: Generation of a global fuel data set using the Fuel Characteristic Classification System, *Biogeosciences*, 13, 2061–2076, <https://doi.org/10.5194/bg-13-2061-2016>, <https://www.biogeosciences.net/13/2061/2016/>, 2016.
- Prentice, I. C., Kelley, D. I., Foster, P. N., Friedlingstein, P., Harrison, S. P., and Bartlein, P. J.: Modeling fire and the terrestrial carbon balance, *Global Biogeochemical Cycles*, 25, <https://doi.org/10.1029/2010GB003906>, <https://agupubs.onlinelibrary.wiley.com/doi/abs/10.1029/2010GB003906>, 2011.



- Rabin, S. S., Magi, B. I., Shevliakova, E., and Pacala, S. W.: Quantifying regional, time-varying effects of cropland and pasture on vegetation fire, *Biogeosciences*, 12, 6591–6604, <https://doi.org/10.5194/bg-12-6591-2015>, 2015.
- Rabin, S. S., Melton, J. R., Lasslop, G., Bachelet, D., Forrest, M., Hantson, S., Kaplan, J. O., Li, F., Mangeon, S., Ward, D. S., Yue, C., Arora, V. K., Hickler, T., Kloster, S., Knorr, W., Nieradzik, L., Spessa, A., Folberth, G. A., Sheehan, T., Voulgarakis, A., Kelley, D. I., Prentice, I. C., Sitch, S., Harrison, S., and Arneth, A.: The Fire Modeling Intercomparison Project (FireMIP), phase 1: experimental and analytical protocols with detailed model descriptions, *Geoscientific Model Development*, 10, 1175–1197, <https://doi.org/10.5194/gmd-10-1175-2017>, <https://www.geosci-model-dev.net/10/1175/2017/>, 2017a.
- Rabin, S. S., Melton, J. R., Lasslop, G., Bachelet, D., Forrest, M., Hantson, S., Kaplan, J. O., Li, F., Mangeon, S., Ward, D. S., Yue, C., Arora, V. K., Hickler, T., Kloster, S., Knorr, W., Nieradzik, L., Spessa, A., Folberth, G. A., Sheehan, T., Voulgarakis, A., Kelley, D. I., Prentice, I. C., Sitch, S., Harrison, S., and Arneth, A.: Supplement of: The Fire Modeling Intercomparison Project (FireMIP), phase 1: experimental and analytical protocols with detailed model descriptions, *Geoscientific Model Development*, 10, 1175–1197, <https://doi.org/10.5194/gmd-10-1175-2017-supplement>, <http://www.geosci-model-dev.net/10/1175/2017/gmd-10-1175-2017-supplement.pdf>, 2017b.
- Randerson, J. T., Chen, Y., van der Werf, G. R., Rogers, B. M., and Morton, D. C.: Global burned area and biomass burning emissions from small fires, *J. Geophys. Res. Biogeosciences*, 117, G04012, <https://doi.org/10.1029/2012JG002128>, <http://doi.wiley.com/10.1029/2012JG002128>, 2012.
- Rasul, G. and Thapa, G. B.: Shifting cultivation in the mountains of South and Southeast Asia: regional patterns and factors influencing the change, *Land Degradation & Development*, 14, 495–508, <https://doi.org/10.1002/ldr.570>, <http://dx.doi.org/10.1002/ldr.570>, 2003.
- Reick, C. H., Raddatz, T., Brovkin, V., and Gayler, V.: Representation of natural and anthropogenic land cover change in MPI-ESM, *Journal of Advances in Modeling Earth Systems*, 5, 459–482, <https://doi.org/10.1002/jame.20022>, <http://doi.wiley.com/10.1002/jame.20022>, 2013.
- Sage, R. F. and Kubien, D. S.: The temperature response of C3 and C4 photosynthesis, *Plant, Cell & Environment*, 30, 1086–1106, <https://doi.org/10.1111/j.1365-3040.2007.01682.x>, <https://onlinelibrary.wiley.com/doi/abs/10.1111/j.1365-3040.2007.01682.x>, 2007.
- Scott, A. C., Bowman, D. M. J. S., Bond, W. J., Pyne, S. J., and Alexander, M. E.: *Fire on Earth: An Introduction*, Wiley-Blackwell, Hoboken, New Jersey, USA, 2014.
- Sitch, S., Smith, B., Prentice, I. C., Arneth, A., Bondeau, A., Cramer, W., Kaplan, J. O., Levis, S., Lucht, W., Sykes, M. T., Thonicke, K., and Venevsky, S.: Evaluation of ecosystem dynamics, plant geography and terrestrial carbon cycling in the LPJ dynamic global vegetation model, *Global Change Biology*, 9, 161–185, <https://doi.org/10.1046/j.1365-2486.2003.00569.x>, <https://onlinelibrary.wiley.com/doi/abs/10.1046/j.1365-2486.2003.00569.x>, 2003.
- Smith, B., Prentice, I. C., and Sykes, M. T.: Representation of vegetation dynamics in the modelling of terrestrial ecosystems: comparing two contrasting approaches within European climate space, *Global Ecology and Biogeography*, 10, 621–637, <https://doi.org/10.1046/j.1466-822X.2001.t01-1-00256.x>, <https://onlinelibrary.wiley.com/doi/abs/10.1046/j.1466-822X.2001.t01-1-00256.x>, 2001.
- Smith, B., Wärlind, D., Arneth, A., Hickler, T., Leadley, P., Siltberg, J., and Zaehle, S.: Implications of incorporating N cycling and N limitations on primary production in an individual-based dynamic vegetation model, *Biogeosciences*, 11, 2027–2054, <https://doi.org/10.5194/bg-11-2027-2014>, <https://www.biogeosciences.net/11/2027/2014/>, 2014.
- Stocks, B. J., Mason, J. A., Todd, J. B., Bosch, E. M., Wotton, B. M., Amiro, B. D., Flannigan, M. D., Hirsch, K. G., Logan, K. A., Martell, D. L., and Skinner, W. R.: Large forest fires in Canada, 1959–1997, *Journal of Geophysical Research: Atmospheres*, 107, <https://doi.org/10.1029/2001JD000484>, <http://dx.doi.org/10.1029/2001JD000484>, 2002.



- Syphard, A. D., Radeloff, V. C., Hawbaker, T. J., and Stewart, S. I.: Conservation Threats Due to Human-Caused Increases in Fire Frequency in Mediterranean-Climate Ecosystems, *Conservation Biology*, 23, 758–769, <https://doi.org/10.1111/j.1523-1739.2009.01223.x>, <http://dx.doi.org/10.1111/j.1523-1739.2009.01223.x>, 2009.
- van Marle, M. J. E., Kloster, S., Magi, B. I., Marlon, J. R., Daniiau, A.-L., Field, R. D., Arneth, A., Forrest, M., Hantson, S., Kehrwald, N. M., Knorr, W., Lasslop, G., Li, F., Mangeon, S., Yue, C., Kaiser, J. W., and van der Werf, G. R.: Historic global biomass burning emissions based on merging satellite observations with proxies and fire models (1750–2015), *Geoscientific Model Development Discussions*, 2017, 1–56, <https://doi.org/10.5194/gmd-2017-32>, <http://www.geosci-model-dev-discuss.net/gmd-2017-32/>, 2017.
- Vanni re, B., Blarquez, O., Rius, D., Doyen, E., Br ucher, T., Colombaroli, D., Connor, S., Feurdean, A., Hickler, T., Kaltenrieder, P., Lemmen, C., Leys, B., Massa, C., and Olofsson, J.: 7000-year human legacy of elevation-dependent European fire regimes, *Quaternary Science Reviews*, 132, 206–212, <https://doi.org/10.1016/j.quascirev.2015.11.012>, <http://linkinghub.elsevier.com/retrieve/pii/S0277379115301773>, 2016.
- Veira, A., Lasslop, G., and Kloster, S.: Wildfires in a warmer climate: Emission fluxes, emission heights, and black carbon concentrations in 2090-2099, *Journal of Geophysical Research: Atmospheres*, 121, 3195–3223, <https://doi.org/10.1002/2015JD024142>, <http://doi.wiley.com/10.1002/2015JD024142>, 2016.
- Veraverbeke, S., Rogers, B., L. Goulden, M., R. Jandt, R., E. Miller, C., B. Wiggins, E., and T. Randerson, J.: Lightning as a major driver of recent large fire years in North American boreal forests, *Nature Climate Change*, 7, 529–534, 2017.
- Wand, S. J. E., Midgley, G. F., Jones, M. H., and Curtis, P. S.: Responses of wild C4 and C3 grass (Poaceae) species to elevated atmospheric CO2 concentration: a meta-analytic test of current theories and perceptions, *Global Change Biology*, 5, 723–741, <https://doi.org/10.1046/j.1365-2486.1999.00265.x>, <https://onlinelibrary.wiley.com/doi/abs/10.1046/j.1365-2486.1999.00265.x>, 2001.
- Wang, Z., Chappellaz, J., Park, K., and Mak, J. E.: Large Variations in Southern Hemisphere Biomass Burning During the Last 650 Years, *Science*, 330, 1663–1666, <https://doi.org/10.1126/science.1197257>, <http://www.sciencemag.org/cgi/doi/10.1126/science.1197257>, 2010.
- Ward, D. S., Kloster, S., Mahowald, N. M., Rogers, B. M., Randerson, J. T., and Hess, P. G.: The changing radiative forcing of fires: global model estimates for past, present and future, *Atmospheric Chemistry and Physics*, 12, 10 857–10 886, <https://doi.org/10.5194/acp-12-10857-2012>, <https://www.atmos-chem-phys.net/12/10857/2012/>, 2012.
- Wenzel, S., Cox, P. M., Eyring, V., and Friedlingstein, P.: Projected land photosynthesis constrained by changes in the seasonal cycle of atmospheric CO2, *Nature*, 538, 499–501, <https://doi.org/10.1038/nature19772>, <http://www.nature.com/articles/nature19772>, 2016.
- Wigley, B. J., Bond, W. J., and Hoffman, M. T.: Thicket expansion in a South African savanna under divergent land use: local vs. global drivers?, *Global Change Biology*, 16, 964–976, <https://doi.org/10.1111/j.1365-2486.2009.02030.x>, <http://dx.doi.org/10.1111/j.1365-2486.2009.02030.x>, 2010.
- Williams, R. J., Cook, G. D., Gill, A. M., and Moore, P. H. R.: Fire regime, fire intensity and tree survival in a tropical savanna in northern Australia, *Austral Ecology*, 24, 50–59, <https://doi.org/10.1046/j.1442-9993.1999.00946.x>, <http://doi.wiley.com/10.1046/j.1442-9993.1999.00946.x>, 1999.
- Wooster, M. J., Roberts, G., Perry, G. L. W., and Kaufman, Y. J.: Retrieval of biomass combustion rates and totals from fire radiative power observations: FRP derivation and calibration relationships between biomass consumption and fire radiative energy release, *Journal of Geophysical Research*, 110, D24 311, <https://doi.org/10.1029/2005JD006318>, <http://doi.wiley.com/10.1029/2005JD006318>, 2005.
- Yue, C., Ciais, P., Cadule, P., Thonicke, K., Archibald, S., Poulter, B., Hao, W. M., Hantson, S., Mouillot, F., Friedlingstein, P., Maignan, F., and Viovy, N.: Modelling the role of fires in the terrestrial carbon balance by incorporating SPITFIRE into the global vegetation



model ORCHIDEE – Part 1: simulating historical global burned area and fire regimes, *Geoscientific Model Development*, 7, 2747–2767, <https://doi.org/10.5194/gmd-7-2747-2014>, <https://www.geosci-model-dev.net/7/2747/2014/>, 2014.

5 Yue, C., Ciais, P., Cadule, P., Thonicke, K., and van Leeuwen, T. T.: Modelling the role of fires in the terrestrial carbon balance by incorporating SPITFIRE into the global vegetation model ORCHIDEE – Part 2: Carbon emissions and the role of fires in the global carbon balance, *Geoscientific Model Development*, 8, 1321–1338, <https://doi.org/10.5194/gmd-8-1321-2015>, <https://www.geosci-model-dev.net/8/1321/2015/>, 2015.

Yue, C., Ciais, P., Zhu, D., Wang, T., Peng, S. S., and Piao, S. L.: How have past fire disturbances contributed to the current carbon balance of boreal ecosystems?, *Biogeosciences*, 13, 675–690, <https://doi.org/10.5194/bg-13-675-2016>, <https://www.biogeosciences.net/13/675/2016/>, 2016.